IEEE Access
Multidisciplinary | Rapid Review | Open Access Journal

Received 22 November 2024, accepted 16 December 2024, date of publication 23 December 2024,
date of current version 31 December 2024.

Digital Object Identifier 10.1109/ACCESS.2024.3521249

RESEARCH ARTICLE

Beyond Pairwise Interactions: Higher-Order Q-Analysis of fMRI-Based Brain Functional Networks in Patients With Major Depressive Disorder

SEMEN A. KURKIN[1,2], NIKITA M. SMIRNOV[1], ROSITSA PAUNOVA[3], SEVDALINA KANDILAROVA[3], DROZDSTOY STOYANOV[3], LARISA MAYOROVA[2], AND ALEXANDER E. HRAMOV[1,2]

[1]Baltic Center for Neurotechnology and Artificial Intelligence, Immanuel Kant Baltic Federal University, 236041 Kaliningrad, Russia
[2]Federal Research and Clinical Center of Intensive Care Medicine and Rehabilitology, 107031 Solnechnogorsk, Russia
[3]Department of Psychiatry and Medical Psychology, Research Institute, Medical University of Plovdiv, 4002 Plovdiv, Bulgaria

Corresponding author: Semen A. Kurkin (kurkinsa@gmail.com)

The work of Semen A. Kurkin, Nikita M. Smirnov, and Alexander E. Hramov was supported by Russian Science Foundation in the part of the Data Analysis under Grant 23-71-30010. The work of Rositsa Paunova, Sevdalina Kandilarova, and Drozdstoy Stoyanov was supported by the Research and Innovation Program for the Development of MU-PLOVDIV—(Strategic Program for Innovations and Research Development Plovdiv (SPIRD)-Medical University Plovdiv (MUP)), European Union-NextGenerationEU in the part of Experimental Works.

This work involved human subjects or animals in its research. Approval of all ethical and experimental procedures and protocols was granted by the Ethics Committee of the Medical University of Plovdiv under Application No. 2/19.04.2018, and performed in line with the Declaration of Helsinki.

ABSTRACT Major depressive disorder (MDD) is associated with complex disruptions in brain function, yet the underlying neural mechanisms remain incompletely understood. Traditional approaches to studying functional brain networks have primarily focused on pairwise interactions between brain regions, offering valuable insights into basic connectivity. However, such methods often fail to capture the complexity of higher-order interactions that are critical for understanding integrative processes in the brain. This study aims to address this gap by applying Q-analysis, a mathematical framework that extends beyond pairwise interactions, to fMRI-derived brain networks to investigate higher-order interactions and structural organization in individuals with MDD compared to healthy controls (HCs). Our analysis revealed significant alterations in the topology of brain networks in MDD patients, characterized by a lower maximum topology level and an increased prevalence of isolated edges and chains at the pairwise interaction level. The substantia nigra area demonstrated a higher topological dimension in MDD, suggesting its greater integration into disrupted network structures, potentially reflecting dopaminergic dysfunction associated with the disorder. Additionally, the consensus networks at higher topology levels indicated distinct network configurations between MDD patients and HCs, with the former exhibiting a single q-connected component primarily involving limbic, cerebellar, and occipital-temporal regions. We identified significant disruptions in the higher-order organizational structures of the brain, characterized by reduced topological diversity and complexity, fewer and less connected cliques, and altered involvement of key brain regions in MDD: the increased engagement of the limbic structures such as the substantia nigra, parahippocampal gyrus, and hippocampus, and decreased involvement of the cerebellum, the occipital and temporal lobes. Our study introduces a novel approach to understanding MDD pathophysiology through the lens of higher-order network structures, offering potential avenues for more targeted diagnostic and therapeutic strategies.

The associate editor coordinating the review of this manuscript and approving it for publication was Hocine Cherifi.

INDEX TERMS Higher-order interactions, fMRI, major depressive disorder, functional brain network, Q-analysis, clique, structure vectors.

I. INTRODUCTION

Functional networks (FNs) have emerged as a powerful framework for describing and analyzing neuronal processes in the brain. These networks offer critical insights into how different brain regions interact to facilitate cognitive and behavioral functions [1], [2]. Constructing a brain network model through functional connectivity involves identifying statistical dependencies between time series data associated with different brain regions, as obtained from functional magnetic resonance imaging (fMRI). Traditional approaches to studying brain FNs primarily focus on pairwise interactions, treating the network as a collection of all possible pairwise combinations of brain regions [3], [4], [5]. From a mathematical perspective, these functional brain networks are represented as graphs with nodes and edges, whose topological properties are analyzed using metrics derived from complex network theory [6], [7], [8]. These metrics have proven sensitive enough to differentiate between healthy individuals and patients with neurological disorders, thus facilitating diagnostic applications based on reconstructed fMRI-based brain FNs. For instance, graph characteristics such as mean node strength, clustering coefficient, and the number of edges have shown significant predictive value in classifying patients with major depressive disorder (MDD) based on functional network measures [9], [10].

While this pairwise interaction-based method has substantially advanced our understanding of brain connectivity, it often fails to capture the complexity of the brain's intrinsic mechanisms, which are fundamentally higher-order and involve large-scale network interactions [11], [12], [13], [14]. Higher-order interactions (HOIs)—relationships involving three or more nodes simultaneously—reflect the brain's capacity to perform its functions through the coordinated activity of multiple regions, leading to the formation of higher-order network structures such as simplicial complexes or hypergraphs [15], [16], [17]. These HOI-based network structures are essential for understanding the brain's integrative processes, as they represent more than just the sum of individual pairwise interactions. Therefore, exploring these higher-order structures is crucial for gaining a deeper understanding of the brain's functional organization [18], [19]. Even in the simplest model network systems, incorporating higher-order interactions results in significant qualitative and quantitative changes in system dynamics [20], [21], [22]. Consequently, the formation of HOI structures in brain FNs may serve as a critical diagnostic marker for understanding changes in brain function in patients with neurological disorders.

Q-analysis provides a robust framework for investigating these higher-order interactions within brain FNs [13], [16], [23]. By leveraging this approach, researchers can uncover and analyze complex network structures that are not readily apparent through pairwise analysis alone. In the paper, we propose and apply a novel mathematical tool to examine the unique organizational features of functional brain networks. Notably, this study marks the first systematic application of Q-analysis to address a socially significant problem: investigating disruptions in the functional brain network associated with the development of major depressive disorder. Understanding these disruptions is paramount for advancing our knowledge of MDD pathophysiology and could potentially guide the development of more effective diagnostic and therapeutic strategies.

II. METHODS

The pipeline of the research paradigm is presented schematically in Fig. 1. A detailed description of all steps and methods is presented below.

A. FMRI PROCEDURE AND DATASET PREPARATION

1) SUBJECTS

We enrolled a total of 164 participants, including 94 individuals without any known psychiatric conditions (healthy controls, HC group) and 70 patients with major depressive disorder (MDD group). Each participant underwent assessment by experienced psychiatrists, including the administration of the Mini International Neuropsychiatric Interview [24] and the Montgomery—Åsberg Depression Rating Scale (MADRS) [25], [26]. Exclusion criteria for both groups included a history of comorbid psychiatric conditions, autoimmune diseases, neurological disorders, previous head trauma, or the presence of metal implants incompatible with MRI scans.

There were no significant differences between the two groups in terms of mean age, sex distribution, or level of education. However, as expected, patients had significantly higher MADRS scores compared to the healthy controls (see Table 1).

2) MR SCANNING AND IMAGE PROCESSING

The MR scanning procedure was performed on a 3T MRI system (GE Discovery 750w). The protocol included a high-resolution structural scan (Sag 3D T1) with a slice thickness of 1 mm, matrix 256 × 256, TR (relaxation time) 7.2 s, TE (echo time) 2. 3 s, and flip angle 12°, FOV 24, resting state functional scan — with slice thickness 3 mm, matrix 64 × 64, repetition time — 2000 ms, echo time — 30 ms, flip angle 90°, 192 volumes [27].

The functional data were preprocessed with SPM 12 software [28] in a standard way [29]. The functional images of each participant were first realigned, co-registered with the high-resolution anatomical image, and normalized to standard MNI space. Parameters for the realignment step were the following: quality 0.9, separation 4,

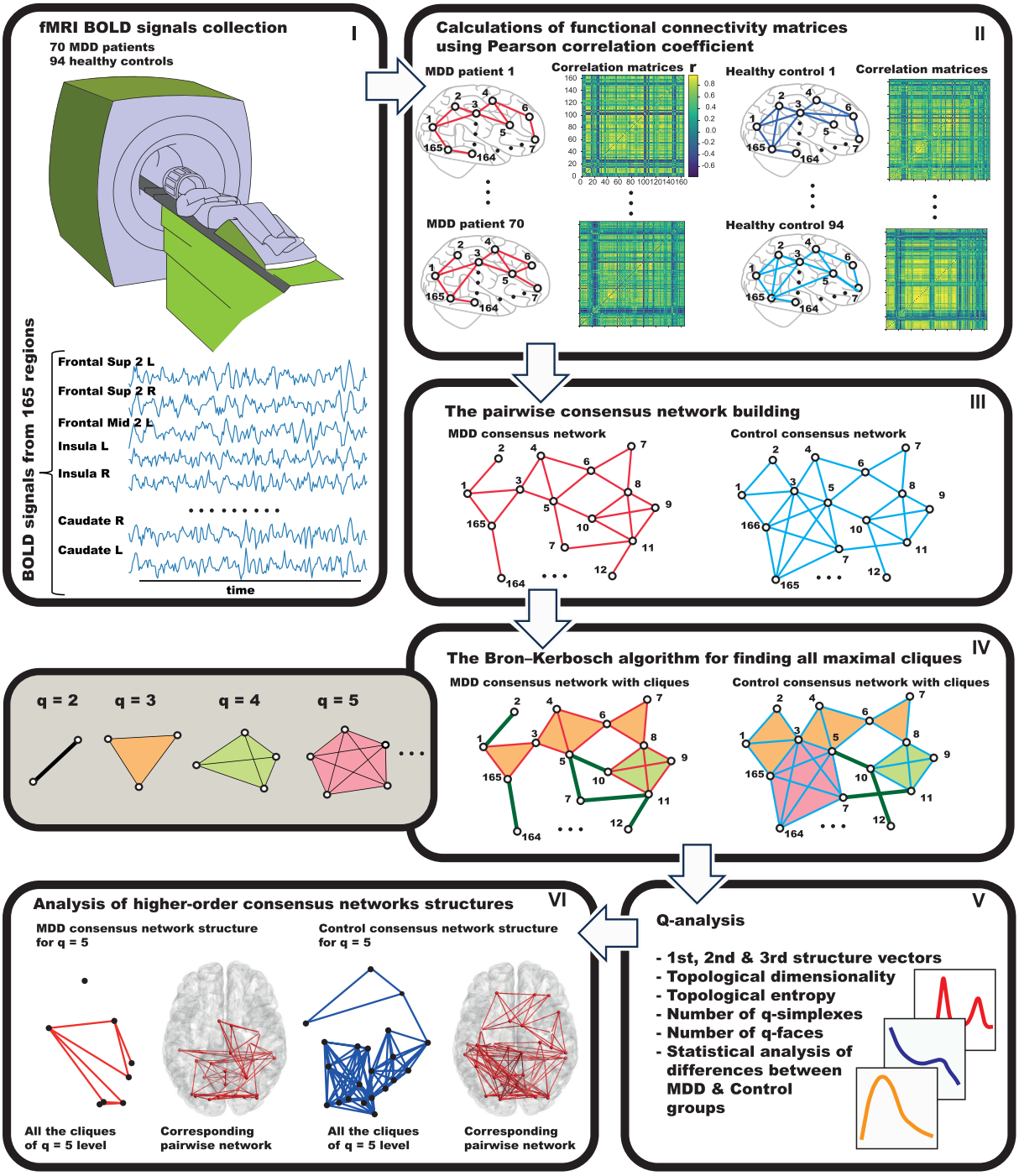

FIGURE 1. Flowchart of the research. (I) Experimental procedure of BOLD signal recording during fMRI with qualitative visualization of time series obtained for 165 brain regions according to the AAL3 brain atlas. (II) Calculation of functional connectivity matrices based on estimation of Pearson correlation coefficients and visualization of corresponding binarized brain networks. (III) Construction of the consensus networks for the MDD and control groups. (IV) Application of the Bron-Kerbosch algorithm to find all maximal cliques (simplices) in the consensus networks; the inset shows the q-cliques for $q = 2, 3, 4$, and 5, which are color-coded in the figure. (V) Q-analysis: the calculation of the specific characteristics. (VI) Visualization and analysis of higher-order structures in the consensus networks.

no smoothing, 2nd degree B-spline interpolation, no wrap, 12×12 basis function, regularization 1 with medium factor, without Jacobian deformations, 5 iterations, average Taylor expansion point. In addition, the default pipeline of the program included a motion correction step for each patient. The co-registration method was set to Normalized Mutual Information. The MNI normalization parameters were as follows: bias regularization 0.0001, bias FWHM 60 mm cutoff, affine regularization ICBM European brain template, warping regularization, no smoothing, sampling distance 3.

TABLE 1. Demographic and clinical characteristics of the considered groups: HC – the group of healthy controls, MDD – the group of patients with major depressive disorder.

	HC ($n = 94$)	MDD ($n = 70$)	Significance
Age (mean ± SD)	40.6 ± 11.8	41.0 ± 13.2	0.961^a
Sex (M/F)	41/53	27/44	0.996^b
Education (secondary/higher)	6/89	7/63	$> 0.999^b$
MADRS score (mean ± SD)	2.0 ± 2.6	29.5 ± 6.0	$< 0.001^a$

SD — Standard Deviation, ^{a}Two-sample Kolmogorov-Smirnov nonparametric test, $^b\chi^2$ — test, MADRS — Montgomery–Åsberg Depression Rating Scale.

As a result, we obtained voxel-level blood oxygen level dependent (BOLD) signals.

3) RECONSTRUCTION OF BRAIN FUNCTIONAL NETWORK

The brain volume was parcellated into 165 regions (see Fig. 1, panel I) according to the automated anatomical labeling atlas AAL3 [30]. We chose the AAL3 atlas because of its widespread use in functional network analysis and optimal level of detail [31]. To assess the connectivity between pairs of brain regions (the so-called, connectivity matrix), we calculated the average BOLD time series $x_i(t)$ for each of 165 brain parcellations (nodes), detrended them, and estimated Pearson correlation coefficients for all pairs of the averaged parcellation activities [10]. The resulting connectivity matrix represents the functional brain network (see Fig. 1, panel II). We then performed a p-value-based binarization of the functional brain networks: we keep only significant connections that had a p-value in the Pearson correlation of less than 0.05.

4) CONSENSUS NETWORKS CALCULATION

To minimize intersubject variability, we utilized the concept of a consensus network (see Fig. 1, panel III), initially introduced for fMRI-based functional networks in [32]. The primary principle of constructing a consensus network involves identifying the common connections that appear in the majority of networks within each group. To create the consensus network, we first eliminate all insignificant connections (with $p > 0.05$) and then retain only those connections that are found in 95% of subjects within the respective group (HC or MDD). These thresholds ($p > 0.05$ and 95%) are standard in statistical analysis.

The consensus network effectively represents the group-specific network structure, thereby mitigating the problem of intersubject variability. By focusing on a single, group-specific network pattern, this approach eliminates the need to consider individual variations in brain connectivity. In addition, the consensus network approach eliminates the need to select a threshold to filter out weak connections, as all significant connections are included in the consensus network. This avoids the potential biases associated with thresholding, which can inadvertently exclude potentially meaningful connections.

B. Q-ANALYSIS

To study higher-order structures in functional brain networks, we used the Q-analysis [16], [33]. Q-analysis is an algebraic topology approach based on identifying and counting all cliques in the network and studying the connections between them. A clique of size (order) q is the complete graph of q vertices, so that every two different vertices in the clique are adjacent (the examples of cliques for $q = 2, 3, 4$, and 5 are shown in the inset in 0. Two cliques C_r and C_q of the orders r, q can be connected by sharing some vertices; the structure formed by the shared vertices represents a common face of both cliques. If for $r < q$ all vertices of C_r belong to C_q, then the clique C_r represents a face of the order r in the clique C_q.

We used the Bron-Kerbosch algorithm [34] to identify all maximal cliques in the obtained consensus networks (see Section II-A4). Based on this information, we then found how different cliques were connected to each other via shared faces to form the higher order structures (clique complexes). The overall hierarchical organization of the graph can be quantified by three structure vectors [16], [23], [35], [36] with components along different topology levels $q = 1, 2, 3, \ldots q_{max}$, where q_{max} is the order of the largest clique in the network. These structure vectors were computed as follows:

- The first structure vector (FSV): $\mathbf{Q} = \{Q_0, Q_1, \ldots Q_{q_{max}-1}, Q_{q_{max}}\}$, where Q_q is the number of q-connected components; a q-connected component is any clique of order $\geq q$ or a set of such cliques connected via common faces of order $r \geq q$. If cliques in a set are connected via a common face of order $r < q$, such cliques are considered as separate components.
- The second structure vector (SSV): $\mathbf{N_s} = \{n_0, n_1, \ldots n_{q_{max}-1}, n_{q_{max}}\}$, where n_q is the number of cliques from the level q upwards.
- The third structure vector (TSV): the component $\hat{Q}_q = 1 - Q_q/n_q$ quantifies the degree of connectedness among cliques at the topology level q.

We also evaluated the topological dimension of nodes and the topological entropy introduced in [23]. The topological dimension $dimQ_i$ of a node i is defined as the number of cliques of all orders in which the corresponding node participates. In fact, the topological dimension is a generalization of the node degree, taking into account higher-order interactions.

Topological entropy of a topology level q was calculated as follows:

$$S_Q(q) = -\frac{\sum_i p_q^i \log p_q^i}{\log M_q}, \quad (1)$$

where p_q^i is the node's occupation probability of the q-level,

$$p_q^i = \frac{K_q^i}{\sum_i K_q^i}, \tag{2}$$

K_q^i is the number of cliques of the order q in which a node i participates, and the normalization factor M_q is the number of nodes that have a non-zero entry at the level q in the entire graph. Thus, the topological entropy measures the degree of cooperation between nodes. The nodes that form an isolated clique result in a higher entropy than the nodes that share different cliques at a given level, resulting in a decrease in entropy [23].

In addition, we computed the number of cliques g and the number of common faces f at different levels q.

All of the above features provide a measure of the global architecture of the graph corresponding to a consensus network. In particular, we can identify all higher-order brain network structures (cliques) with the nodes (brain regions) that form them, as well as how these cliques are connected to each other by sharing specific groups of nodes.

We used our custom Python package "Q-analysis toolkit": https://github.com/pakrentos/q-analysis.

C. STATISTICAL ANALYSIS

To address the multiple comparisons problem and a possible non-normality of the distributions of the Q-analysis measures (structure vectors, entropy, number of cliques, and number of common faces) across the topology levels q, we used an extended consensus network-based permutation test. This method extends the classical permutation test by incorporating shared structural information across networks within each group and can be described as follows.

$$\text{LetHC} = (HC_1, \ldots, HC_n) \text{and} \text{MDD} = (MDD_1, \ldots, MDD_m)$$

be two samples of size n and m, respectively, representing Q-analysis measures from the HC and MDD groups of networks. To test the null hypothesis H_0 that HC and MDD come from the same distribution, the permutation test is performed as follows [37], [38]:

1) Compute for each topology level q the observed value of the test statistic (see below) for the initial groups HC and MDD, t_o.
2) Generate permutations of the combined sample $(HC_1, \ldots, HC_n, MDD_1, \ldots, MDD_m)$.
3) For each permutation j:
   - Divide the permuted sample into two groups $A^{(j)}$ and $B^{(j)}$ of size n and m.
   - Compute for each topology level q the test statistic (see below) t_j.
4) Compute the p-value as the proportion of permutations where the distribution values of the test statistic exceed the observed value of the test statistic: $|t_j| \geq |t_o|$ for a two-sided test.

This non-parametric method determines the statistical significance of differences between two groups by generating a null distribution against which the observed difference is compared.

The consensus network-based test statistic is calculated as follows:

1) Compute consensus networks for each group in the comparison (see Section II-A4).
2) Compute the distributions of the Q-analysis measures across the topology levels q for these consensus networks.
3) Find the difference in the measures between the two groups for each topology level q.
4) Use these differences as the test statistic for the permutation test.

Thus, the test statistic is calculated as the difference between the Q-analysis measures derived from the consensus networks of each group. We calculate differences for multiple measures, and each is treated independently in the subsequent statistical analysis. Permutation testing process then involves randomly reassigning samples to groups, recalculating the test statistic, and constructing a permutation distribution for each metric. The significance level was set at 0.05. The permutation distribution contained 10000 samples.

This method allows us to assess the statistical significance of the observed differences in Q-analysis measures between groups, while taking into account the shared structural information within each group.

We performed the similar statistical procedure for the topological dimension across nodes.

To analyze the statistical significance of the difference between the structure vectors of the groups at the macro level, we calculated the modulus of difference between the corresponding vectors and then applied the similar permutation-based procedure.

We used the Python libraries numpy and scipy and the "Q-analysis toolkit" (https://github.com/pakrentos/q-analysis) for statistical analysis.

D. VISUALIZATION OF CHARACTER HIGHER-ORDER NETWORK STRUCTURES

To illustrate the topology of a network of cliques of order q for each topology level q, we created a multilayer decomposition of the original consensus networks for the MDD and HC groups. Each layer in such a representation corresponds to a particular topology level q, and the nodes on each layer represent cliques of order q, while the connections represent common faces of different orders $r < q$ between pairs of connected cliques. The coordinate of a node corresponding to a clique was calculated as the centroid of the corresponding clique. We used the Python library matplotlib for the visualization of the multilayer decomposition.

We analyzed and visualized the hypoactivated and hyperactivated connections in the particular q-connected component in the MDD group compared to the HC group. We define the hyperactivated connections as those that are present in the q-connected component of the MDD group, but are missing in the consensus network of the HC group. On the contrary,

the hypoactivated connections are present in the q-connected component of the HC group, but are missing in the consensus network of the MDD group. To quantitatively characterize the hypoactivated and hyperactivated subnetworks, we calculated the node degree measure for the regions included in these subnetworks. We emphasize that the node degree is calculated considering only the connections included in the corresponding subnetwork, so the same region may have different node degrees in the two given subnetworks. To visualize the q-connected components and the hypoactivated/hyperactivated subnetworks in a brain, we used the Python libraries mne-connectivity and netplotbrain.

In this section, we have described the details of the fMRI procedure and data preprocessing, including the technique of reconstructing functional brain networks, as well as the basics of Q-analysis and the statistical and visualization methods used.

III. RESULTS

A. MULTILAYER DECOMPOSITION

Figure 2 shows the multilayer representation of the consensus networks of the HC and MDD groups. This figure illustrates the diverse composition of cliques of different order and variants of their combination into larger components, which allows us to qualitatively analyze higher-order structures in brain FNs, as well as to demonstrate the differences between groups at different levels of HOI. While the classical representation of a network by pairwise interactions does not uncover fully connected higher-order network structures (see e.g. the pictograms with red networks on the brain in the margins of Fig. 2), the decomposition into distinct layers of cliques allows to elegantly and clearly identify and illustrate all higher-order structures separately at each topology level.

The $q = 1$ topology level corresponds to pairwise interactions and shows the original consensus networks. It can be seen that the density of connections in the HC network is higher than in the MDD network. At $q = 2$, there is an essentially higher number of cliques in the MDD group, indicating a higher number of isolated edges and chains in the characteristic functional network of the patient group. At higher levels, the network of the HC group has a larger number of cliques for most levels q, as well as a larger number of connections between cliques. Importantly, the maximum clique dimensionality q_{max} for the MDD group is 9—and at this level of topology the networks of both groups have one clique each—while for the HC group $q_{max} = 11$.

B. Q-ANALYSIS MEASURES OF THE CONSENSUS NETWORKS

1) TOPOLOGICAL DIMENSIONS AND NETWORK HUBS

We computed the topological dimensions $dimQ_i$ of all nodes for the HC and MDD consensus networks and sorted them according to their dimensions. As a result, we identified the top 10 regions with maximum dimensions for both groups — the so-called hubs of the networks, taking into account the HOIs (see Table 2). Thus, these hub regions are involved in a maximum number of higher-order structures. On average, the topological dimension is higher for the HC group, and the maximum dimension for the HC group is 24, while for the MDD group it is 19. The composition and order of brain areas in the top-10 lists differs between groups. Unique to the list of the HC group (marked in green in Table 2) are the areas of the occipital cortex, and for the MDD group (marked in red) — the hippocampus. Common to both lists (marked in blue) are areas of the temporal cortex, postcentral gyrus, fusiform and cerebellum.

Applying a permutation-based statistical procedure to the distributions of topological dimension across nodes, we found that this measure was significantly greater ($p = 0.0105$) in the MDD group for the Substantia nigra (pars compacta) region. This node was involved in 3 cliques of the 2^{nd} order in the MDD group as opposed to a single clique of the 2^{nd} order in the HC group (see Table 3).

Thus, all the nodes of the cliques containing the Substantia nigra (pars compacta) region are midbrain regions, with the first clique being the same in both groups and the MDD group containing two additional 2-cliques (see Table 3).

2) STRUCTURE VECTORS AND TOPOLOGICAL ENTROPY

We analyzed the difference between the structure vectors of the MDD and HC groups.

At the macro level, there were the significant effects in the modulus of difference between the first structure vectors ($p = 0.0453$, see Table 4) and the third structure vectors ($p = 0.0308$) of the groups. Thus, on average, regardless of the topology level q, there was a difference between the groups in the number of q-connected components and the degree of connectedness among cliques in the consensus functional networks.

At the level of individual topology levels, we found the following significant effects for the structure vectors (see the dependencies of the components of the structure vectors in Fig. 3; significant effects are highlighted with red asterisks under the abscissa axis):

- The 2^{nd} component of the first structure vector was significantly higher in the MDD group, and the 10^{th} and 11^{th} components were significantly higher in the HC group.
- The 9^{th}, 10^{th}, and 11^{th} components of the second structure vector were significantly higher in the HC group.
- The 2^{nd}, 8^{th}, 9^{th}, and 10^{th} components of the third structure vector were significantly higher in the HC group.

The revealed statistically significant difference in the 2^{nd} component of the FSV implies the presence of a greater number of separate isolated edges (2-cliques) in the MDD group, compared to the HC group (see also Fig. 2, $q = 2$). This conclusion was also supported by the significantly higher number of cliques at the $q = 2$ level in the corresponding dependence $g(q)$ in Fig. 3. The significant effects at the levels $q = 10$ and 11 were a consequence of

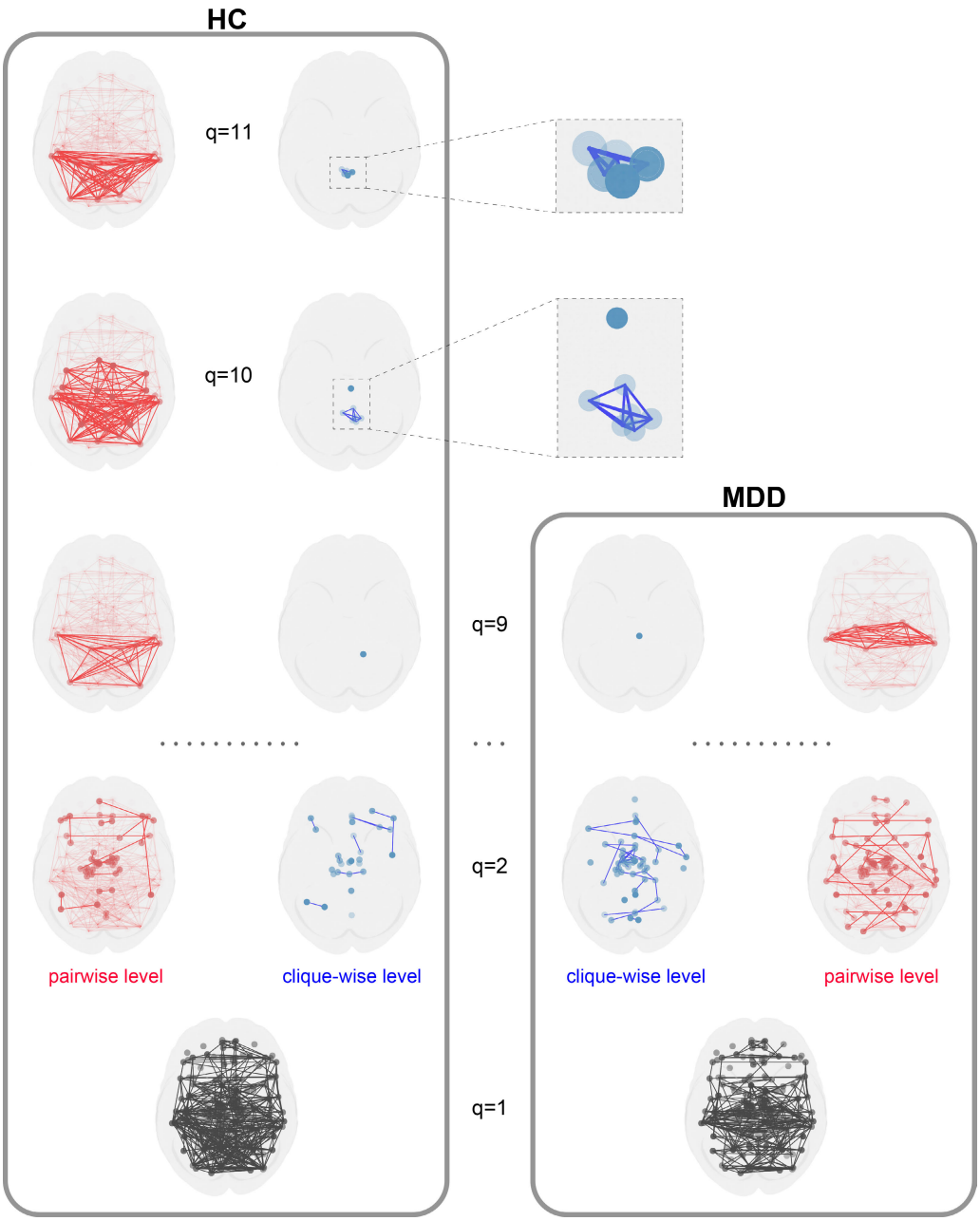

FIGURE 2. Multilayer representation of the original consensus networks for the HC and MDD groups on a brain (superior view). Each layer represents a particular topology level q. The topology level $q = 1$, shown in black, corresponds to pairwise interactions and illustrates the original consensus networks. The blue nodes on each layer in the middle part of the figure represent cliques of order q corresponding to that layer, and the blue edges represent shared faces of different orders $r < q$ between pairs of connected cliques. Thus, each layer reflects the topology of a network of cliques of order q. In the side parts of the figure, the pairwise networks corresponding to the networks of cliques at the level q are highlighted in the dark red, while the light red networks show the entire original consensus networks. In the MDD group, there are no cliques of order $q > 9$. For the HC group, we show the zoomed clique networks of orders $q = 10$ and $q = 11$. For compactness, we show only those topology levels ($q = 1, 2, 9, 10, 11$) where there are qualitative differences between the groups; an illustration of all levels is provided in the Supplementary Material S1.

the fact that the order of the largest clique q_{max} was 9 in the MDD group and 11 in the HC group.

The general trend in the change of the components of the first and second structure vectors for both groups is a monotonous decrease in their magnitudes with increasing q. This trend is violated in the HC group at the level $q = 10$, where the FSV shows a sharp increase. The essential increase in the number of q-connected components at this level indicates a relatively large number of cliques of order $q \geq 10$ (see also the increase in the number of cliques for $q = 10$ and 11 in the dependence $g(q)$ in Fig. 3), and that many of them are connected by common faces of order $r = 9$

TABLE 2. Top-10 hubs with the highest topological dimension for the HC and MDD groups with their rank (rank:HC and rank:MDD) and topological dimensions ($dimQ_{HC}$ and $dimQ_{MDD}$) in the HC and MDD consensus networks. Some of the nodes are present in both top-10 lists (they are marked with blue color), and some are present in only one of the top-10 lists of the groups — this results in 15 rows in the table. Nodes specific to the HC group are marked with green color, those specific to the MDD group are marked with red color.

rank:HC	$\mathrm{dimQ_{HC}}$	Hub name	$\mathrm{dimQ_{MDD}}$	rank:MDD
1	24	Fusiform R	16	3
2	23	Calcarine R	7	11
3	20	Temporal Mid R	19	1
4	16	Postcentral L	8	9
5	16	Cerebellum 4 5 L	14	4
6	15	Occipital Sup L	6	13
7	15	Calcarine L	6	14
8	13	Cerebellum 6 R	6	15
9	13	Temporal Inf L	7	10
10	12	Occipital Inf L	2	71
14	10	Temporal Mid L	16	2
24	7	Vermis 4 5	10	7
29	7	Temporal Inf R	10	6
48	4	Hippocampus R	8	8
64	3	Fusiform L	11	5

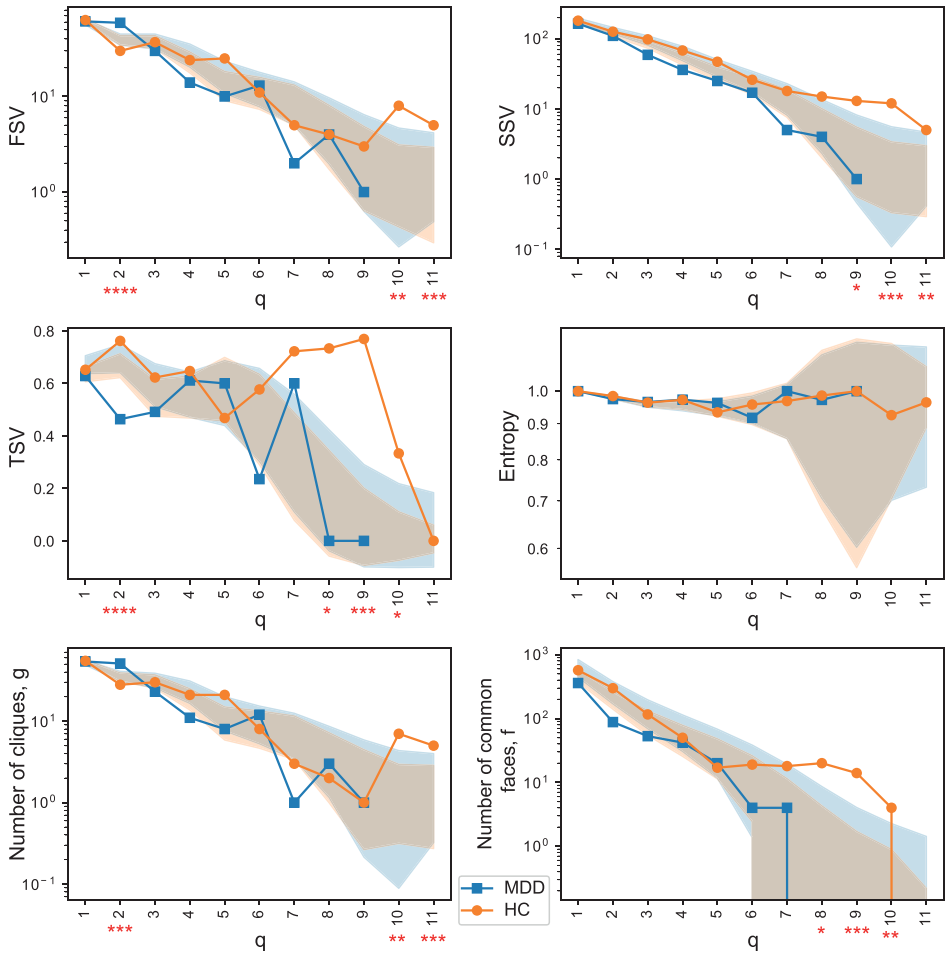

FIGURE 3. The components of three structure vectors (FSV, SSV, TSV), topological entropy, number of cliques and common faces plotted against the topology level q for the consensus networks of the MDD and HC groups. Asterisks denote q levels for which characteristics are statistically significantly different between groups: '*' — $p < 0.05$, '**' — $p < 0.025$, '***' — $p < 0.01$, '****' — $p < 0.001$. The shaded regions indicate the mean ± SD of the corresponding permutation distributions.

(see also the dependence of the number of common faces $f(q)$ in Fig. 3), thus forming a small number of the components at the level $q = 9$. When moving to the level $q = 10$, these cliques become disconnected and form a larger number

TABLE 3. The composition of the cliques containing the substantia nigra (pars compacta) region in the consensus networks of the MDD and HC groups. For this region, a significant difference in topological dimension was found between the groups. This region is involved in three cliques for the MDD group, while it is involved in only one clique for the HC group.

#	Nodes involved in the cliques, MDD group	Nodes involved in the clique, HC group
1	[Substantia nigra (pars compacta) R, Substantia nigra (pars reticulata) R]	[Substantia nigra (pars compacta) R, Substantia nigra (pars reticulata) R]
2	[Substantia nigra (pars compacta) R, Red nucleus R]	
3	[Substantia nigra (pars compacta) R, Ventral tegmental area R]	

TABLE 4. Statistical significance of the modulus of difference between the HC and MDD groups of the first, second, and third structure vectors estimated by the permutation-based procedure.

Measure	p-value
$\lvert\mathbf{Q}^{MDD} - \mathbf{Q}^{HC}\rvert$	0.0453
$\lvert\mathbf{N_s}^{MDD} - \mathbf{N_s}^{HC}\rvert$	0.2052
$\lvert\hat{\mathbf{Q}}^{MDD} - \hat{\mathbf{Q}}^{HC}\rvert$	0.0308

of components. Meanwhile, there are no cliques of this dimension in MDD.

The significant effects in the third structure vector show that the degree of connectedness among cliques is higher in the HC group at levels $q = 2, 8, 9$, and 10. In general, this means that there are more cliques of the specified orders and higher in the consensus network of the HC group, but they form larger higher-order connected structures, which is reflected in the smaller number of q-connected components.

We found no significant effects for the topological entropy measure (see Fig. 3). At the same time, an important feature of the topological entropy dependence is the position of its minimum, since it indicates the geometric forms through which the nodes are mostly interconnected. We can see that for the MDD consensus network these are 6-cliques. For the HC group, there are two local minima: the first one corresponds to the 5-cliques and the second one—to the 10-cliques. Thus, in the HC group, the network nodes are more connected through higher dimensional structures.

C. HIGHER-ORDER NETWORK STRUCTURES

The previous analysis showed that the main differences in the properties of higher-order interactions in the functional networks of the groups start at the level $q = 9$. In order to disentangle which patterns of structural organization of the networks lead to such differences, we constructed and analyzed q-connected components at the level $q = 9$ for the HC and MDD groups (see Fig. 4). There are three q-connected components in the consensus network of the HC group and one q-connected component in the consensus network of the MDD group. Thus, the HC group exhibits a richer and more diverse composition of higher-order network structures.

Fig. 4 shows that the q-connected components represent functionally closely interconnected brain regions. Interestingly, the presented components are characterized by a rather high degree of localization, i.e. they contain predominantly regions from neighboring brain areas. The first and second q-connected components ($q = 9$) of the HC group overlap to a greater extent and contain the following regions: areas of the occipital and temporal lobes, cerebellum, and vermis. The third component includes the precentral and postcentral gyri, supplementary motor area, paracentral lobule, and parietal areas. The only q-connected component ($q = 9$) of the MDD group contains areas of the limbic system, cerebellum, occipital, and temporal lobes.

It can be seen that the differences between the groups in higher-order network structures are not only in the number and size of such structures, but also in their composition, i.e., their localization in the brain. The main distinctions between the components of the MDD and HC groups are the participation of areas of the limbic system in the MDD component, as well as the absence of the pre- and postcentral gyri, the supplementary motor area, and most of the occipital, parietal, and cerebellar areas. This conclusion is also supported by the analysis of the topological dimensions of brain regions in Section III-B1.

Notably, different regions within the components of the HC group are characterized by different degrees of involvement in the cliques (see in Fig. 4 the color scale on the connectograms corresponding to the local topological dimension of the nodes). Some regions are involved in a large number of cliques—a maximum of 12—and are therefore important hubs for the formation of higher-order structures in the network. These are mainly areas of the occipital and parietal cortex, as well as the cerebellum. At the same time, some nodes are involved in only a few cliques—in terms of network organization, they are at the ''periphery'' of the network.

Thus, the differences between the q-connected components of the groups reflect the disruptions in higher-order network organization in the MDD group.

D. HYPOACTIVATED AND HYPERACTIVATED SUBNETWORKS IN BRAIN FNS

In order to reveal the disrupted brain subnetworks in the MDD group, we contrasted the described q-connected components for $q = 9$ with the consensus networks of the groups (for details, see Section II-D) and thus discovered the hypoactivated and hyperactivated subnetworks in the MDD group (see Fig. 5). Specifically, the consensus network of the MDD group lacks the connections present in the hypoactivated subnetwork, preventing the formation of higher-order structures. In contrast, connections from the hyperactivated subnetwork are redundant in the MDD group's consensus network compared to the HC group's consensus network, resulting in a higher-order redundant structure.

The hypoactivated subnetwork involves the following regions: areas of the occipital, temporal, parietal lobes, cerebellum and vermis, and the precentral and postcentral gyri (for details, see Fig. 5 and tables in Supplementary Material S3). The hyperactivated subnetwork includes: areas of the temporal lobe and cerebellum, hippocampus, and

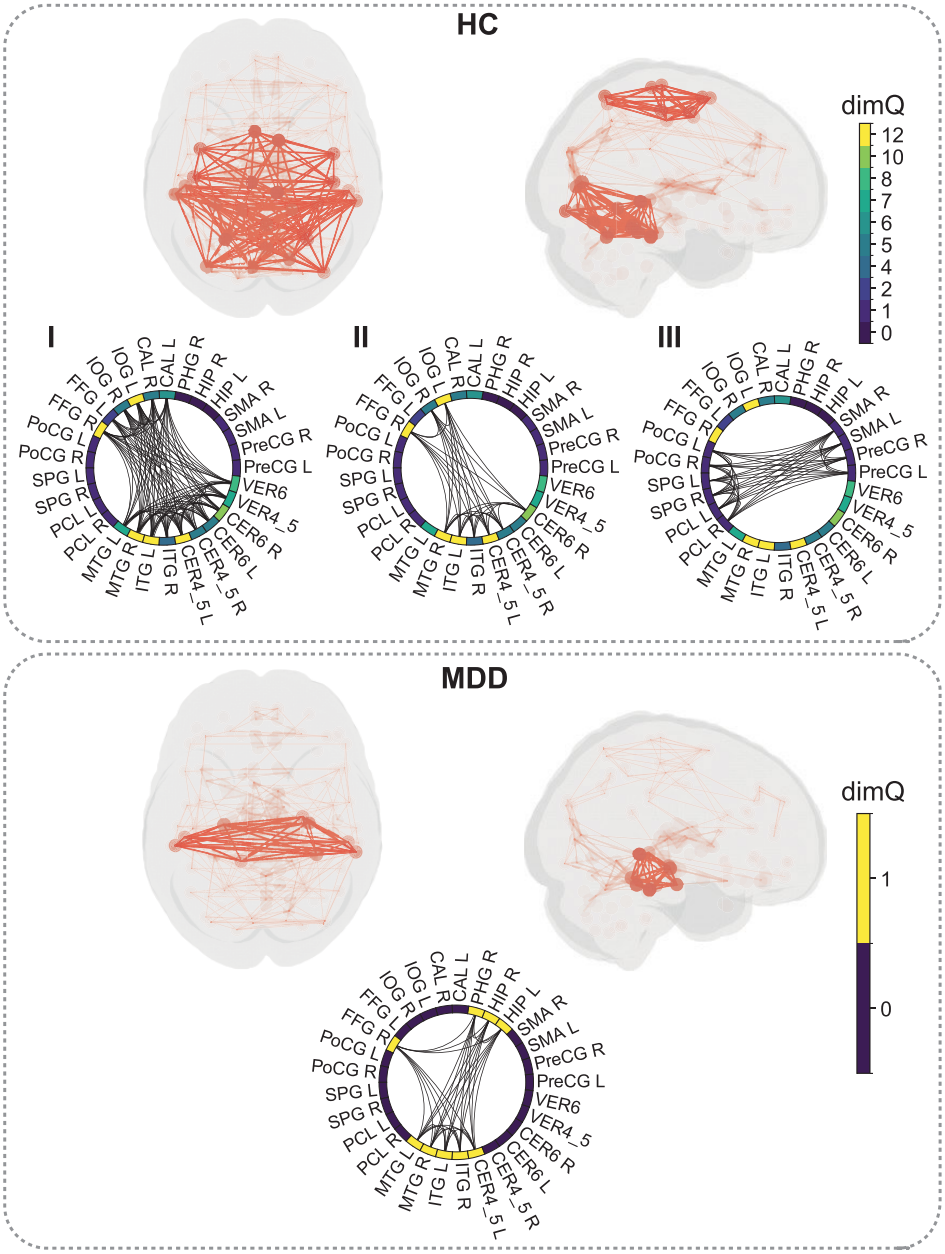

FIGURE 4. Dark red subnetworks in the brain illustrate q-connected components at the level $q = 9$ for the HC and MDD groups (superior and side views); the light red networks show the entire original consensus networks. A q-connected component is any clique of order $\geq q$ or a set of such cliques connected via common faces of order $r \geq q$. If cliques in a set are connected via a common face of order $r < q$, such cliques are considered as separate components. At the level $q = 9$, there are three q-connected components in the consensus network of the HC group and one q-connected component in the consensus network of the MDD group. These q-connected components are shown separately in the corresponding connectograms. The color in the connectograms indicates a local topological dimension (*dimQ*) for the regions from the considered q-connected components; the local topological dimension is calculated considering only the cliques included in the considered q-connected components. The list of brain region abbreviations can be found in Section VI. The composition of all components is detailed in the tables in the Supplementary Material S2.

parahippocampal gyrus. These results support the conclusions of Section III-C.

The local degree of a node reflects the level of disruption of a region (see the color scale in Fig. 5). The higher the local degree of a node, the more disrupted connections are associated with that region — such nodes represent disrupted hubs. They are the most critical elements in the breakdown of the formation of normal higher-order network structures in the brain. In the hypoactivated subnetwork, the following are the most important disrupted hubs with local degree $D \geq 5$:

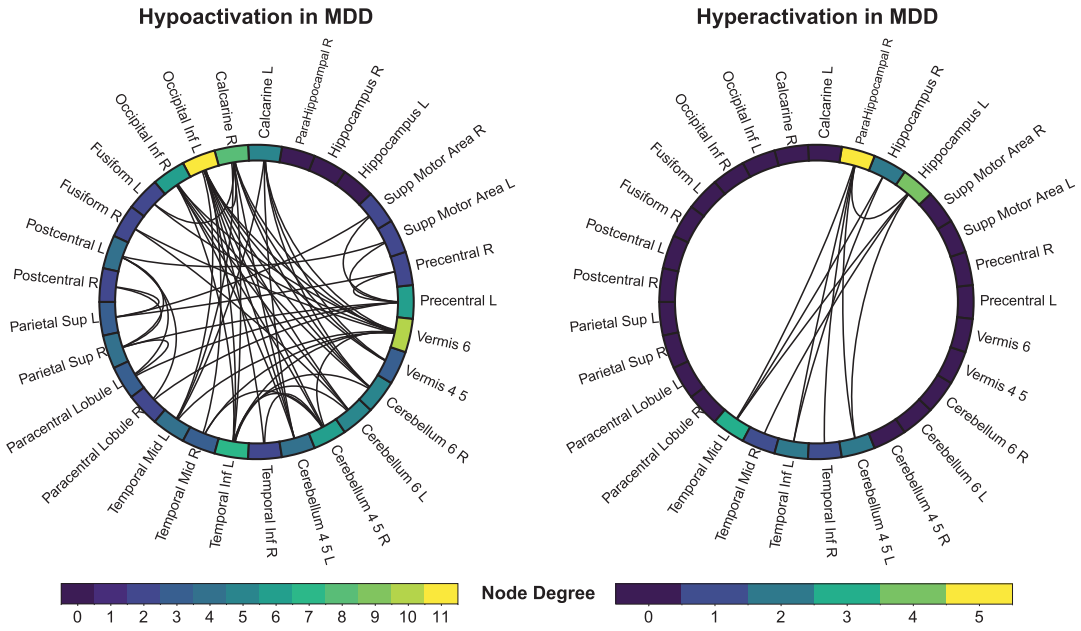

FIGURE 5. Hypoactivated and hyperactivated connections for the MDD group in the q-connected components at the level $q = 9$. Hypoactivated connections are present in the q-connected component of the HC group, but are missing in the consensus network of the MDD group. Hyperactivated connections are present in the q-connected component of the MDD group, but are missing in the consensus network of the HC group. For ease of comparison, the connectograms include all regions (nodes) belonging to either the hypoactivated or hyperactivated subnetwork. The color in the connectograms indicates a node local degree measure for the regions in the hypoactivated and hyperactivated subnetworks; the node local degree is calculated considering only the connections included in the corresponding subnetwork, so the same region has different node degrees in the two given subnetworks. The composition of the hypoactivated and hyperactivated subnetworks is detailed in the tables in the Supplementary Material S3.

left inferior occipital gyrus ($D = 11$), lobule VI of vermis ($D = 10$), right calcarine ($D = 8$), left inferior temporal gyrus ($D = 7$), left precentral gyrus ($D = 6$), right inferior occipital gyrus ($D = 6$), right lobule IV, V of the cerebellar hemisphere ($D = 6$), left calcarine ($D = 5$), and right lobule VI of the cerebellar hemisphere ($D = 5$). In the hyperactivated subnetwork, the major disrupted hubs ($D \geq 3$) are: right parahippocampal gyrus ($D = 5$), left hippocampus ($D = 4$), and left middle temporal gyrus ($D = 3$).

Thus, this section presents the main results of the analysis of the Q-measures of the functional networks of the MDD group, as well as the emerging higher-order network structures and the characteristics of these structures in terms of hypoactivation and hyperactivation of brain subnetworks.

IV. DISCUSSION

In the present study, we employed Q-analysis to investigate disruptions in the functional brain networks associated with major depressive disorder (MDD) from a fundamentally novel perspective. Unlike traditional analyses that focus on individual nodes and pairwise connections, our approach examines higher-order interactions (HOIs) involving multiple brain regions simultaneously. Our analysis revealed disruptions in the brain network of MDD patients, where dysfunctions in pairwise interactions, reflected in hypo- and hyperactivated subnetworks, cascade into perturbations in more complex, higher-order structures, preventing normal cooperative functioning across the brain.

Traditional analysis at the level of pairwise interactions provides valuable insights into which individual connections are disrupted but cannot reveal the extent of damage to larger, more integrated network structures. Although our previous studies demonstrated significant alterations at the pairwise level [9], [10], [29], [32], they lacked a broader view of the structural network abnormalities that may impair cognitive functions. Higher-order structures represent functionally closely connected brain regions that work in concert to facilitate complex cognitive and behavioral processes [13], [39]. Disruptions at this level indicate a fundamental impairment in the brain's ability to integrate information across multiple regions, which may underpin the cognitive and emotional deficits observed in MDD.

A. COMPARISON WITH OTHER APPROACHES FOR RECONSTRUCTING HOIS

Several methodologies exist for reconstructing HOIs from brain activity signals. One approach involves using measures and algorithms that estimate the strength of interactions between multiple brain regions simultaneously, such as O-Information and partial entropy decomposition [40], [41], [42] or LASSO-based methods [43], [44]. While these methods can effectively capture complex interactions in the form of hyperedges, they are often hampered by high computational complexity and challenges in interpreting hypergraphs. To address interpretability, different types of hypergraph expansions are utilized [45], [46], e.g.,

graph models like line and high-order graphs have been employed [44], [47], though this simplification can result in information loss [48].

Another approach involves calculating the ''correlation of correlations'', effectively treating higher-order interactions as correlations between already computed pairwise correlations [49], [50]. This method, however, introduces entanglement and complicates the interpretation and explainability of the results.

The representation of HOIs by cliques, as used in our study, offers distinct advantages in terms of simplicity and interpretability. By transitioning from pairwise interactions to higher-order structures using pairwise correlation estimates, cliques effectively capture functionally cohesive brain regions without the substantial computational burden and interpretive challenges associated with other methods. This approach has proven particularly valuable in clinical applications, as demonstrated in studies of schizophrenia [51], neurodegeneration [12], and attention deficit hyperactivity disorder (ADHD) [52].

Recent developments in the field have also explored directed hypergraph approaches, which attempt to incorporate the directionality of information flow in higher-order interactions; in particular, such an approach has been applied to the identification of MDD [53]. In addition, researchers have successfully applied HOI analysis to various neuroimaging modalities, including EEG data [54], demonstrating the versatility of higher-order approaches in capturing complex neural dynamics that can be used to diagnose various neurological disorders. These advances suggest that while pairwise analyses have historically dominated the field, modern higher-order methods are increasingly recognized as essential tools for understanding brain organization in both health and disease.

B. ADVANTAGES AND LIMITATIONS OF Q-ANALYSIS

Q-analysis proves to be an effective tool for describing the higher-order structures (cliques) due to its combinatorial nature [16], [23], [33]. It facilitates the identification of global characteristics, such as structure vectors and entropy, before delving into specific topology levels for a more detailed examination. Importantly, Q-analysis retains all information without loss, making it well-suited for functional networks where all-to-all connections within cliques imply strong functional integration. It can capture both large and small network structures formed by connected cliques. Our use of multilayer decomposition further enhances this analysis, allowing us to visualize and understand how different topology levels contribute to the overall network structure.

However, Q-analysis has its limitations. It primarily detects HOIs that satisfy the clique property, meaning all nodes within a clique must be fully interconnected. Consequently, large-scale brain networks that do not form complete cliques may be partially or entirely overlooked by Q-analysis. This inherent constraint suggests that traditional methods, such as Independent Component Analysis (ICA) [55], might be more appropriate for analyzing certain large-scale brain networks that do not conform to the clique structure. Nonetheless, our introduction of multilayer decomposition within Q-analysis allows for a more nuanced exploration of network structures across various topology levels, mitigating some of these limitations.

C. HIGHER-ORDER INTERACTIONS AND NETWORK DISRUPTIONS IN MDD

To our knowledge, this study represents the first application of Q-analysis to MDD, providing novel insights into the higher-order organizational disruptions that characterize the disorder. Our findings reveal that individuals with MDD exhibit reduced topological diversity and complexity in their functional brain networks. Specifically, the MDD group demonstrated a lower maximum topology level ($q_{max} = 9$) compared to healthy controls ($q_{max} = 11$), alongside an increased number of isolated edges and chains at the pairwise level and a diminished number of cliques and inter-clique connections at higher topology levels.

Furthermore, significant alterations were observed in the topological dimensions of specific brain regions. The substantia nigra, for instance, exhibited a higher topological dimension in the MDD group, participating in more cliques compared to the HC group. This finding, along with the marked differences in hub regions between groups, underscores the reorganization of functional networks in MDD. Additionally, the consensus network analysis at the $q = 9$ level highlighted a loss of distinct, high-level functional subnetworks in the MDD group, further illustrating the compromised integration within their brain networks.

Finally, by comparing the q-connected components with the consensus networks of each group, we identified disrupted subnetworks and disrupted hubs in the MDD group. Specifically, the hypoactivated subnetwork included the hubs located in the areas of the occipital, temporal, and parietal lobes, as well as the cerebellum, vermis, and pre- and postcentral gyri. Meanwhile, the hyperactivated subnetwork involved the disrupted hubs in the regions of the temporal lobe and cerebellum, hippocampus, and parahippocampal gyrus. In summary, MDD shows stronger involvement of limbic structures such as the substantia nigra, parahippocampal gyrus, and hippocampus, and weaker involvement of the occipital and temporal lobes and the cerebellum.

These higher-order findings complement our previous pairwise analyses by providing a more holistic view of the network disruptions in MDD. While pairwise analyses identify specific weakened or strengthened connections, the Q-analysis elucidates how these perturbations collectively impact the brain's ability to form and maintain complex, integrated network structures that are essential for cognitive and emotional functioning. This research contributes to the growing body of knowledge on the role of complex network structures in mental health disorders and underscores the potential of Q-analysis as a tool for investigating the intricate dynamics of brain function. Understanding these disruptions

in higher-order interactions may lead to more effective diagnostic tools and therapeutic strategies for MDD.

D. CONTRIBUTION OF THE ANALYSIS TO THE UNDERSTANDING OF DISRUPTIONS IN MDD

Let us discuss our findings in the context of the known results on disruptions in the functional brain network in MDD. The greater involvement of the substantia nigra (SSN) in the functional network of patients with MDD is a significant finding that may offer insights into the neurobiological underpinnings of the disorder. The SSN is traditionally known for its role in the dopaminergic system, particularly in the regulation of movement, reward processing, and motivation [56]. Dysregulation of dopaminergic pathways has long been associated with mood disorders, including MDD, suggesting that the increased involvement of the SSN in the functional brain networks of MDD patients may reflect alterations in these critical neural circuits [57].

In MDD, there is substantial evidence supporting the involvement of dopamine-related dysfunction [58]. Dopamine is a neurotransmitter that plays a crucial role in reward processing, motivation, and the regulation of mood [59]. The SSN, as a major source of dopaminergic neurons projecting to various brain regions, including the striatum and prefrontal cortex, is central to these processes [60]. The observed higher topological dimension of the SSN in the MDD group indicates that this region is more extensively integrated into the brain's functional network in these patients, potentially reflecting compensatory mechanisms or maladaptive changes in response to altered dopaminergic signalling [61]. This interpretation is supported by the presence of a clique involving other dopaminergic brain regions, such as the ventral tegmental area, which was found only in MDD patients.

The greater involvement of the SSN in the functional networks of MDD patients could also be related to the cognitive and affective symptoms characteristic of the disorder. The SSN's increased participation in multiple cliques, or higher-order network structures, suggests that it may play a more prominent role in coordinating activity across different brain regions involved in mood regulation, decision-making, and emotional processing [62]. This could manifest as the characteristic symptoms of MDD, such as anhedonia, reduced motivation, and psychomotor retardation, which are closely linked to disruptions in dopaminergic pathways [63].

Our results are consistent with classical functional connectivity studies that have shown disrupted connectivity in several large-scale resting-state networks, including the default mode network (DMN), salience network (SN), central executive network (CEN), thalamic, limbic, and cerebellar regions [64], [65], [66]. The disruptions of the aforementioned networks have been linked to dysfunctions in several neurotransmitter systems, with most evidence supporting the involvement of both dopaminergic and serotonergic afferent and efferent projections. Dopamine dysregulation has been related to alterations in the sensorimotor network (SMN) via the nigrostriatal pathway, the salience and executive networks via the mesocorticolimbic pathway. Similarly, serotonergic neurons from the raphe nuclei project to regions of the SMN, SN, and DMN [67]. In addition, pharmacoMRI with dopaminergic and antipsychotic drugs has confirmed the effects of dopamine on the activity and functional connectivity of all three networks [68]. Data suggest that 5-HT signalling increases DMN activity while decreasing SMN activity [69], [70].

Numerous studies highlight the involvement of the hippocampus in the pathophysiology of MDD, as part of the limbic system, with reductions in gray matter volume observed in meta-analyses and associated with depressive symptoms in both the general population and medication-free patients [71], [72], [73], [74]. In addition, hippocampal volume has been correlated with depression scores in younger patients [75] and associated with remission rates [76].

FMRI studies underscore the disrupted hippocampal activity and connectivity in MDD, with many studies reporting increased hippocampal activity during negative information processing [75] and decreased activity during interoceptive tasks [77]. While there are mixed reports on hippocampal connectivity [78] —showing both increases and decreases with other brain regions—network measures such as nodal efficiency in the left hippocampus have been negatively correlated with depression severity and positively correlated with improvements in depressive symptoms following antidepressant treatment [79]. In addition, hippocampal connectivity patterns have been associated with declarative memory deficits, a common symptom of depression [80].

Recent research has increasingly focused on demonstrating structural and functional impairments in MDD. However, investigations of alterations in higher-order coupling between structure and function remain limited. Our findings are consistent with previous studies indicating that MDD patients exhibit reduced higher-order coupling in various connections. In addition, one study observed a local rich-hub organization in MDD patients characterized by higher-order coupling in connections between the ventral attention network and the limbic network compared to healthy controls [81]. Furthermore, a recent study showed that patients with MDD exhibit increased structural connectivity-functional connectivity coupling in intermodule connectivity between the ventral attention and limbic networks [82]. This finding may suggest that MDD patients have more rigid, less flexible and less dynamic brain function. The ventral attention network is primarily involved in the monitoring of salient events and the processing and regulation of emotions [83], [84]. It is also known to have strong connections with the limbic network, which plays a critical role in integrating emotional information and evaluating rewards [85], [86].

One of our findings concerns the central role of the cerebellum. In addition to its role in motor control, the cerebellum is also involved in various cognitive and emotional processes. Research has shown that different areas of the cerebellum are associated with specific higher-order

cognitive and emotional processing [87]. These findings are consistent with previous studies that have highlighted the critical role of the cerebellum in depression and its potential connection to core networks [88], [89]. Certain connections may be associated with clinical symptoms of depression, such as slower movement and cognitive changes [90]. In addition, the study suggests that the vermis could serve as a potential biomarker for the diagnosis of MDD due to its connections to the hippocampus, orbitofrontal cortex, and thalamus, all of which are considered critical for mood regulation [91]. In particular, the vermis has been implicated in mediating emotion and cognition [92].

A separate study reiterates the importance of increased cerebellar connectivity with the temporal poles and decreased connectivity with regions within the default mode and executive control networks in adults diagnosed with major depression [93]. In addition, the study suggests that adults with depression have reduced functional connectivity within the cerebellum (primarily involving right lobule VI, left crus I, and bilateral lobule VIIb) compared to healthy individuals.

The DMN, known for its involvement in self-referential activity, episodic memory retrieval, and emotional regulation, has been consistently associated with dysfunction in depression [94], [95], [96]. In addition, connectivity between the cerebellum (including the left crus I and bilateral lobule VIIb) and the CEN showed a reduction in adults diagnosed with major depression. The CEN plays a critical role in cognitive control and decision-making and is known to be impaired in individuals with depression [95]. Previous research has highlighted the involvement of specific cerebellar regions within the CEN in healthy individuals [97].

A recent study used discriminative higher-order network analysis and identified several brain regions that are affected in patients with MDD [98]. These regions include the hippocampus, anterior cingulate gyrus, posterior cingulate gyrus, orbital frontal cortex, and temporal pole. These regions are part of the brain's ''core networks'', including the DMN, salience network, and CEN. These networks support higher cognitive functions and have been implicated in the pathophysiology of depression. The hippocampus, as a component of the DMN, may have a potential role in MDD [99]. The default mode network plays a critical role in consciousness and memory processing in depression and has a strong connection to the limbic system [100].

In a separate study, increased node centralities were observed in MDD patients in the right anterior cingulate gyrus, left posterior cingulate gyrus, right medial superior frontal gyrus, bilateral hippocampus, and bilateral parahippocampal gyrus, which are central regions of the DMN [101]. Specifically, the study showed a negative correlation between the node degree of the right hippocampus and the duration of depression, suggesting that right hippocampal connectivity may progressively decrease during disease progression. As noted above, the hippocampus is involved in memory retrieval and reward; this brain region may play a central role in the pathophysiology of MDD [102]. One study found hippocampal volume loss in first-episode depression through quantitative meta-analysis [103], and this atrophy is positively associated with disease duration [104]. The increased connectivity between regions in the limbic system suggests that bottom-up affective processing may be overprocessed in MDD [105]. Thus, the obtained results elucidate from a network perspective the abnormality of the affective processing system in MDD patients.

Consistent with our research, another study indicates that from a higher-order perspective, MDD patients show a significant reduction in the dynamics of five subnetworks, including the DMN, cognitive control network, bilateral limbic network, and auditory network [106]. Furthermore, they suggest that MDD has a limited impact on the detection of brain communities, but the overlapping brain regions differ between MDD and HC. In addition, other research suggests decreased within-network connectivity in MDD compared to HC in the visual network (VN), sensorimotor network (SMN), and DMN [107]. Furthermore, this study shows that three between-network connections also show significant decreases in MDD: VN-SMN, VN-DAN (dorsal attention network), and SMN-DAN. Some of the observed variations may be due to different clinical characteristics and severity of depression, which may lead to different brain activation patterns and, consequently, different topological properties within brain networks.

Although our findings are largely consistent with previous research, there are some differences between our approach and existing research. As mentioned above, the application of Q-analysis to the study of MDD networks provides a unique perspective on network organization. Consistent with our findings, numerous studies suggest reduced topological diversity and complexity in MDD brain networks [108], [109], [110]. In addition, study [111] found disrupted neural connections, particularly within the prefrontal, sensorimotor, and cerebellar networks. However, unlike our approach, it did not provide specific details regarding hypo- or hyperactivation of these regions. In addition, most of the research focuses on prominent neural networks such as the DMN, SN, and key components of the limbic system [112], [113], [114]. Also, some studies have focused their approach on linking peripheral markers of MDD to network dysfunction [115], [116], which changes the perspective of the approach and may explain the possible inconsistencies in the results. These methodological discrepancies are due to our innovative approach, which allows us to identify weakened or strengthened connections in the organization of brain networks at the level of higher-order interactions.

The identification of disrupted higher-order structures in MDD has significant implications for both our understanding and treatment of the disorder. The revealed reduced topological diversity and complexity suggests that the brain's ability to integrate information across regions is compromised, potentially leading to the cognitive and emotional

deficits observed in MDD patients. Moreover, the altered involvement of specific brain regions, such as the increased role of the substantia nigra and hippocampus alongside the decreased engagement of the occipital and temporal lobes and cerebellum, may inform targeted therapeutic strategies aimed at restoring functional network integrity.

In this section, we compared the developed Q-analysis approach with other approaches for reconstructing HOIs, discussed its advantages and limitations, and the revealed features of higher-order interactions and network disruptions in MDD. We also discussed in detail the contribution of the conducted analysis to the understanding of disruptions in MDD.

V. LIMITATIONS AND FUTURE WORK

As we have mentioned in Section IV-B, the fundamental limitation of Q-analysis is the inability to detect incompletely connected subnetworks, which is conditioned by the clique property. Future studies should use traditional methods, such as Independent Component Analysis (ICA) [55], to complement the obtained results with the analysis of large-scale brain networks that do not conform to the clique structure.

In addition to the limitations of the Q-analysis, there are other caveats to our study. The naturalistic design of the study does not allow the influence of medication to be excluded, as most of the patients were taking different groups of antidepressants. Future studies should investigate the topology of functional networks in unmedicated subgroups.

The obtained results may have limited generalizability due to the sample size and the single-center patient recruitment strategy. To address this limitation, we have initiated three international independent replications in Russia, China, and Portugal.

Moreover, future research should continue to integrate higher-order network analyses with other methodological approaches to further elucidate the complex neurobiological mechanisms of MDD and to develop more effective diagnostic and therapeutic interventions.

VI. CONCLUSION

In summary, our study pioneers the use of Q-analysis to explore higher-order interactions within functional brain networks in individuals with major depressive disorder. We identified significant disruptions in the higher-order organizational structures of the brain, characterized by reduced topological diversity and complexity, fewer and less connected cliques, and altered involvement of key brain regions in MDD: the increased engagement of the limbic structures such as the substantia nigra, parahippocampal gyrus, and hippocampus, and decreased involvement of the cerebellum, the occipital and temporal lobes. These findings provide a deeper understanding of the network-level perturbations underlying MDD and offer complementary insights to traditional pairwise interaction analyses.

In addition, we note that Q-analysis can be applied to a wide range of neurological and psychiatric disorders, as it offers a way to detect and quantify disruptions in the organization of brain networks that underlie various cognitive and behavioral impairments. Furthermore, the combinatorial nature of Q-analysis means that it does not impose strong assumptions about the network structure, making it adaptable to different datasets and scales of analysis. It can reveal subtle changes in network topology that might correspond to disease states, developmental stages, or responses to treatment, thus providing a universal tool for neuroscience research. By shifting the focus from individual connections to the broader patterns of network interaction, Q-analysis opens new avenues for exploring the complexity of brain function and dysfunction in a more comprehensive manner.

ETHICAL STATEMENT

Prior to participation, all individuals provided written informed consent in accordance with the principles outlined in the Declaration of Helsinki. The study protocol was reviewed and approved by the Ethics Committee of the Medical University of Plovdiv (approval number: 2/19.04.2018).

ABBREVIATIONS

The following abbreviations are used in this study:

MDD	Major depressive disorder.
HC	Healthy control.
fMRI	Functional magnetic resonance imaging.
FN	Functional network.
HOIs	Higher-order interactions.
PreCG	Precentral gyrus.
SMA	Supplementary motor area.
CAL	Calcarine fissure.
IOG	Inferior occipital gyrus.
FFG	Fusiform gyrus.
PoCG	Postcentral gyrus.
SPG	Superior parietal gyrus.
PCL	Paracentral lobule.
MTG	Middle temporal gyrus.
ITG	Inferior temporal gyrus.
CER4_5	Lobule IV, V of cerebellar hemisphere.
CER6	Lobule VI of cerebellar hemisphere.
VER4_5	Lobule IV, V of vermis.
VER6	Lobule VI of vermis.
HIP	Hippocampus.
PHG	Parahippocampal gyrus.
AAL	Automatic anatomical labeling atlas.
BOLD	Blood-oxygenation-level-dependent.
SSN	Substantia nigra.
CEN	Central executive network.
DMN	Default mode network.
SN	Salience network.
VN	Visual network.
SMN	Sensorimotor network.
DAN	Dorsal attention network.
ADHD	Attention deficit hyperactivity disorder.
HC	Healthy controls.
SD	Standard deviation.

SUPPLEMENTARY INFORMATION

There are three supplementary files:

- SupplementaryS1 file, which contains an illustration of all levels og the multilayer representation of the original consensus networks for the HC and MDD groups.
- SupplementaryS2 file, which contains the detailed composition (the lists of nodes or brain regions) of all q-connected components at the level $q = 9$ for the HC and MDD groups.
- SupplementaryS3 file, which contains the composition of the hypoactivated and hyperactivated subnetworks for the MDD group in the q-connected components at the level $q = 9$.

REFERENCES

[1] E. Bullmore and O. Sporns, "Complex brain networks: Graph theoretical analysis of structural and functional systems," *Nature Rev. Neurosci.*, vol. 10, no. 3, pp. 186–198, Mar. 2009.

[2] K. J. Friston, "Functional and effective connectivity: A review," *Brain Connectivity*, vol. 1, no. 1, pp. 13–36, Jan. 2011.

[3] S. Smith and T. Nichols, "Threshold-free cluster enhancement: Addressing problems of smoothing, threshold dependence and localisation in cluster inference," *NeuroImage*, vol. 44, no. 1, pp. 83–98, Jan. 2009.

[4] M. Rubinov and O. Sporns, "Complex network measures of brain connectivity: Uses and interpretations," *NeuroImage*, vol. 52, no. 3, pp. 1059–1069, Sep. 2010.

[5] A. E. Hramov, N. S. Frolov, V. A. Maksimenko, S. A. Kurkin, V. B. Kazantsev, and A. N. Pisarchik, "Functional networks of the brain: From connectivity restoration to dynamic integration," *Phys.-Uspekhi*, vol. 64, no. 6, pp. 584–616, Sep. 2021.

[6] S. Boccaletti, V. Latora, Y. Moreno, M. Chávez, and D. Hwang, "Complex networks: Structure and dynamics," *Phys. Rep.*, vol. 424, nos. 4–5, pp. 175–308, Jan. 2006.

[7] O. Sporns, "Structure and function of complex brain networks," *Dialogues Clin. Neurosci.*, vol. 15, no. 3, pp. 247–262, Sep. 2013.

[8] D. S. Bassett and O. Sporns, "Network neuroscience," *Nature Neurosci.*, vol. 20, no. 3, pp. 353–364, Feb. 2017.

[9] A. V. Andreev, S. A. Kurkin, D. Stoyanov, A. A. Badarin, R. Paunova, and A. E. Hramov, "Toward interpretability of machine learning methods for the classification of patients with major depressive disorder based on functional network measures," *Chaos, Interdiscipl. J. Nonlinear Sci.*, vol. 33, no. 6, Jun. 2023, Art. no. 063140.

[10] D. Stoyanov, V. Khorev, R. Paunova, S. Kandilarova, D. Simeonova, A. Badarin, A. Hramov, and S. Kurkin, "Resting-state functional connectivity impairment in patients with major depressive episode," *Int. J. Environ. Res. Public Health*, vol. 19, no. 21, p. 14045, Oct. 2022.

[11] A. Zalesky, A. Fornito, and E. T. Bullmore, "Network-based statistic: Identifying differences in brain networks," *NeuroImage*, vol. 53, no. 4, pp. 1197–1207, Dec. 2010.

[12] O. Sporns, "Contributions and challenges for network models in cognitive neuroscience," *Nature Neurosci.*, vol. 17, no. 5, pp. 652–660, May 2014.

[13] C. Giusti, R. Ghrist, and D. S. Bassett, "Two's company, three (or more) is a simplex: Algebraic-topological tools for understanding higher-order structure in neural data," *J. Comput. Neurosci.*, vol. 41, no. 1, pp. 1–14, Aug. 2016.

[14] R. Herzog, F. E. Rosas, R. Whelan, S. Fittipaldi, H. Santamaria-Garcia, J. Cruzat, A. Birba, S. Moguilner, E. Tagliazucchi, P. Prado, and A. Ibanez, "Genuine high-order interactions in brain networks and neurodegeneration," *Neurobiol. Disease*, vol. 175, Dec. 2022, Art. no. 105918.

[15] U. Braun, A. Schäfer, D. S. Bassett, F. Rausch, J. I. Schweiger, E. Bilek, S. Erk, N. Romanczuk-Seiferth, O. Grimm, L. S. Geiger, L. Haddad, K. Otto, S. Mohnke, A. Heinz, M. Zink, H. Walter, E. Schwarz, A. Meyer-Lindenberg, and H. Tost, "Dynamic brain network reconfiguration as a potential schizophrenia genetic risk mechanism modulated by NMDA receptor function," *Proc. Nat. Acad. Sci. USA*, vol. 113, no. 44, pp. 12568–12573, Nov. 2016.

[16] M. Andjelković, B. Tadić, and R. Melnik, "The topology of higher-order complexes associated with brain hubs in human connectomes," *Sci. Rep.*, vol. 10, no. 1, p. 17320, Oct. 2020.

[17] S. Boccaletti, P. De Lellis, C. I. del Genio, K. Alfaro-Bittner, R. Criado, S. Jalan, and M. Romance, "The structure and dynamics of networks with higher order interactions," *Phys. Rep.*, vol. 1018, pp. 1–64, May 2023.

[18] A. E. Sizemore, C. Giusti, A. Kahn, J. M. Vettel, R. F. Betzel, and D. S. Bassett, "Cliques and cavities in the human connectome," *J. Comput. Neurosci.*, vol. 44, no. 1, pp. 115–145, Feb. 2018.

[19] F. Battiston, G. Cencetti, I. Iacopini, V. Latora, M. Lucas, A. Patania, J.-G. Young, and G. Petri, "Networks beyond pairwise interactions: Structure and dynamics," *Phys. Rep.*, vol. 874, pp. 1–92, Aug. 2020.

[20] S. Majhi, M. Perc, and D. Ghosh, "Dynamics on higher-order networks: A review," *J. Roy. Soc. Interface*, vol. 19, no. 188, Mar. 2022, Art. no. 20220043.

[21] Y. Zhang, M. Lucas, and F. Battiston, "Higher-order interactions shape collective dynamics differently in hypergraphs and simplicial complexes," *Nature Commun.*, vol. 14, no. 1, p. 1605, Mar. 2023.

[22] M. S. Anwar, N. Frolov, A. E. Hramov, and D. Ghosh, "Self-organized bistability on globally coupled higher-order networks," *Phys. Rev. E, Stat. Phys. Plasmas Fluids Relat. Interdiscip. Top.*, vol. 109, no. 1, Jan. 2024, Art. no. 014225.

[23] M. Andjelković, N. Gupte, and B. Tadić, "Hidden geometry of traffic jamming," *Phys. Rev. E, Stat. Phys. Plasmas Fluids Relat. Interdiscip. Top.*, vol. 91, no. 5, May 2015, Art. no. 052817.

[24] D. V. Sheehan, Y. Lecrubier, K. H. Sheehan, P. Amorim, J. Janavs, E. Weiller, T. Hergueta, R. Baker, and G. C. Dunbar, "The mini-international neuropsychiatric interview (M.I.N.I.): The development and validation of a structured diagnostic psychiatric interview for DSM-IV and ICD-10," *J. Clin. Psychiatry*, vol. 59, p. 22, Jan. 1998.

[25] M. Müller, "Differentiating moderate and severe depression using the montgomery–Åsberg depression rating scale (MADRS)," *J. Affect. Disorders*, vol. 77, no. 3, pp. 255–260, Dec. 2003.

[26] S. A. Montgomery and M. Åsberg, "A new depression scale designed to be sensitive to change," *Brit. J. Psychiatry*, vol. 134, no. 4, pp. 382–389, Apr. 1979.

[27] D. Stoyanov, S. Kandilarova, K. Aryutova, R. Paunova, A. Todeva-Radneva, A. Latypova, and F. Kherif, "Multivariate analysis of structural and functional neuroimaging can inform psychiatric differential diagnosis," *Diagnostics*, vol. 11, no. 1, p. 19, Dec. 2020.

[28] *Spm12*. Accessed: Apr. 12, 2024. [Online]. Available: http://www.fil.ion.ucl.ac.uk/spm

[29] E. N. Pitsik, V. A. Maximenko, S. A. Kurkin, A. P. Sergeev, D. Stoyanov, R. Paunova, S. Kandilarova, D. Simeonova, and A. E. Hramov, "The topology of fMRI-based networks defines the performance of a graph neural network for the classification of patients with major depressive disorder," *Chaos, Solitons Fractals*, vol. 167, Feb. 2023, Art. no. 113041.

[30] E. T. Rolls, C.-C. Huang, C.-P. Lin, J. Feng, and M. Joliot, "Automated anatomical labelling atlas 3," *NeuroImage*, vol. 206, Feb. 2020, Art. no. 116189.

[31] M. L. Stanley, M. N. Moussa, B. M. Paolini, R. G. Lyday, J. H. Burdette, and P. J. Laurienti, "Defining nodes in complex brain networks," *Frontiers Comput. Neurosci.*, vol. 7, p. 169, Nov. 2013.

[32] A. N. Pisarchik, A. V. Andreev, S. A. Kurkin, D. Stoyanov, A. A. Badarin, R. Paunova, and A. E. Hramov, "Topology switching during window thresholding fMRI-based functional networks of patients with major depressive disorder: Consensus network approach," *Chaos: Interdiscipl. J. Nonlinear Sci.*, vol. 33, no. 9, Sep. 2023, Art. no. 093122.

[33] R. H. Atkin, "From cohomology in physics to Q-connectivity in social science," *Int. J. Man-Mach. Stud.*, vol. 4, no. 2, pp. 139–167, Apr. 1972.

[34] C. Bron and J. Kerbosch, "Algorithm 457: Finding all cliques of an undirected graph," *Commun. ACM*, vol. 16, no. 9, pp. 575–577, Sep. 1973.

[35] J. Jonsson, *Simplicial Complexes Graphs*, vol. 1928. Cham, Switzerland: Springer, 2008.

[36] S. Maletić, M. Rajković, and D. Vasiljević, "Simplicial complexes of networks and their statistical properties," in *Proc. 8th Int. Conf. Comput. Sci.*, Kraków, Poland, Jan. 2008, pp. 568–575.

[37] P. Good, *Permutation Tests: A Practical Guide to Resampling Methods for Testing Hypotheses* (Springer Series in Statistics). New York, NY, USA: Springer, Jan. 2000.

[38] E. Maris and R. Oostenveld, "Nonparametric statistical testing of EEG- and MEG-data," *J. Neurosci. Methods*, vol. 164, no. 1, pp. 177–190, Aug. 2007.

[39] O. Sporns, "Network attributes for segregation and integration in the human brain," *Current Opinion Neurobiol.*, vol. 23, no. 2, pp. 162–171, Apr. 2013.

[40] M. Gatica, R. Cofré, P. A. M. Mediano, F. E. Rosas, P. Orio, I. Diez, S. P. Swinnen, and J. M. Cortes, "High-order interdependencies in the aging brain," *Brain Connectivity*, vol. 11, no. 9, pp. 734–744, Nov. 2021.

[41] L. Sparacino, L. Faes, G. Mijatović, G. Parla, V. Lo Re, R. Miraglia, J. de Ville de Goyet, and G. Sparacia, "Statistical approaches to identify pairwise and high-order brain functional connectivity signatures on a single-subject basis," *Life*, vol. 13, no. 10, p. 2075, Oct. 2023.

[42] T. F. Varley, M. Pope, M. Grazia, Joshua, and O. Sporns, "Partial entropy decomposition reveals higher-order information structures in human brain activity," *Proc. Nat. Acad. Sci. USA*, vol. 120, no. 30, Jul. 2023, Art. no. e2300888120.

[43] H. Guo, Y. Li, Y. Xu, Y. Jin, J. Xiang, and J. Chen, "Resting-state brain functional hyper-network construction based on elastic net and group lasso methods," *Frontiers Neuroinform.*, vol. 12, p. 25, May 2018.

[44] H. Guo, X. Huang, C. Wang, H. Wang, X. Bai, and Y. Li, "High-order line graphs of fMRI data in major depressive disorder," *Med. Phys.*, vol. 51, no. 8, pp. 5535–5549, Aug. 2024.

[45] S. Agarwal, K. Branson, and S. Belongie, "Higher order learning with graphs," in *Proc. 23rd Int. Conf. Mach. Learn. (ICML)*, 2006, pp. 17–24.

[46] S. Bandyopadhyay, K. Das, and M. N. Murty, "Hypergraph attention isomorphism network by learning line graph expansion," in *Proc. IEEE Int. Conf. Big Data (Big Data)*, Dec. 2020, pp. 669–678.

[47] T. S. Evans and R. Lambiotte, "Line graphs of weighted networks for overlapping communities," *Eur. Phys. J. B*, vol. 77, no. 2, pp. 265–272, Sep. 2010.

[48] M. Hein, S. Setzer, L. Jost, and S. S. Rangapuram, "The total variation on hypergraphs-learning on hypergraphs revisited," in *Proc. Adv. Neural Inf. Process. Syst.*, vol. 26, 2013, pp. 1–11.

[49] Y. Zhou, L. Qiao, W. Li, L. Zhang, and D. Shen, "Simultaneous estimation of low- and high-order functional connectivity for identifying mild cognitive impairment," *Frontiers Neuroinform.*, vol. 12, p. 3, Feb. 2018.

[50] F. Zhao, H. Zhang, I. Rekik, Z. An, and D. Shen, "Diagnosis of autism spectrum disorders using multi-level high-order functional networks derived from resting-state functional MRI," *Frontiers Hum. Neurosci.*, vol. 12, p. 184, May 2018.

[51] S. M. Plis, J. Sui, T. Lane, S. Roy, V. P. Clark, V. K. Potluru, R. J. Huster, A. Michael, S. R. Sponheim, M. P. Weisend, and V. D. Calhoun, "High-order interactions observed in multi-task intrinsic networks are dominant indicators of aberrant brain function in schizophrenia," *NeuroImage*, vol. 102, pp. 35–48, Nov. 2014.

[52] X. Xi, J. Li, Z. Wang, H. Tian, and R. Yang, "The effect of high-order interactions on the functional brain networks of boys with ADHD," *Eur. Phys. J. Special Topics*, vol. 233, no. 4, pp. 817–829, Jun. 2024.

[53] J. Liu, W. Yang, Y. Ma, Q. Dong, Y. Li, and B. Hu, "Effective hyper-connectivity network construction and learning: Application to major depressive disorder identification," *Comput. Biol. Med.*, vol. 171, Mar. 2024, Art. no. 108069.

[54] F. Zhao, H. Pan, N. Li, X. Chen, H. Zhang, N. Mao, and Y. Ren, "High-order brain functional network for electroencephalography-based diagnosis of major depressive disorder," *Frontiers Neurosci.*, vol. 16, Aug. 2022, Art. no. 976229.

[55] V. D. Calhoun, J. Liu, and T. Adalı, "A review of group ICA for fMRI data and ICA for joint inference of imaging, genetic, and ERP data," *NeuroImage*, vol. 45, no. 1, pp. S163–S172, Mar. 2009.

[56] A. Björklund and S. B. Dunnett, "Dopamine neuron systems in the brain: An update," *Trends Neurosciences*, vol. 30, no. 5, pp. 194–202, May 2007.

[57] E. J. Nestler and W. A. Carlezon, "The mesolimbic dopamine reward circuit in depression," *Biol. Psychiatry*, vol. 59, no. 12, pp. 1151–1159, Jun. 2006.

[58] P. Belujon and A. A. Grace, "Dopamine system dysregulation in major depressive disorders," *Int. J. Neuropsychopharmacol.*, vol. 20, no. 12, pp. 1036–1046, Dec. 2017.

[59] W. Schultz, "Multiple dopamine functions at different time courses," *Annu. Rev. Neurosci.*, vol. 30, no. 1, pp. 259–288, Jul. 2007.

[60] S. N. Haber and B. Knutson, "The reward circuit: Linking primate anatomy and human imaging," *Neuropsychopharmacology*, vol. 35, no. 1, pp. 4–26, Jan. 2010.

[61] H. S. Mayberg, "Modulating dysfunctional limbic-cortical circuits in depression: Towards development of brain-based algorithms for diagnosis and optimised treatment," *Brit. Med. Bull.*, vol. 65, no. 1, pp. 193–207, Mar. 2003.

[62] L. Wang, D. F. Hermens, I. B. Hickie, and J. Lagopoulos, "A systematic review of resting-state functional-MRI studies in major depression," *J. Affect. Disorders*, vol. 142, nos. 1–3, pp. 6–12, Dec. 2012.

[63] M. T. Treadway and D. H. Zald, "Reconsidering anhedonia in depression: Lessons from translational neuroscience," *Neurosci. Biobehavioral Rev.*, vol. 35, no. 3, pp. 537–555, Jan. 2011.

[64] R. H. Kaiser, J. R. Andrews-Hanna, T. D. Wager, and D. A. Pizzagalli, "Large-scale network dysfunction in major depressive disorder: A meta-analysis of resting-state functional connectivity," *JAMA Psychiatry*, vol. 72, no. 6, pp. 603–611, 2015.

[65] J. Brakowski, S. Spinelli, N. Dörig, O. G. Bosch, A. Manoliu, M. G. Holtforth, and E. Seifritz, "Resting state brain network function in major depression—Depression symptomatology, antidepressant treatment effects, future research," *J. Psychiatric Res.*, vol. 92, pp. 147–159, Sep. 2017.

[66] V. S. Khorev, S. A. Kurkin, G. Zlateva, R. Paunova, S. Kandilarova, M. Maes, D. Stoyanov, and A. E. Hramov, "Disruptions in segregation mechanisms in fMRI-based brain functional network predict the major depressive disorder condition," *Chaos, Solitons Fractals*, vol. 188, Nov. 2024, Art. no. 115566.

[67] B. Conio, M. Martino, P. Magioncalda, A. Escelsior, M. Inglese, M. Amore, and G. Northoff, "Opposite effects of dopamine and serotonin on resting-state networks: Review and implications for psychiatric disorders," *Mol. Psychiatry*, vol. 25, no. 1, pp. 82–93, Jan. 2020.

[68] G. Shafiei, Y. Zeighami, C. A. Clark, J. T. Coull, A. Nagano-Saito, M. Leyton, A. Dagher, and B. Mišić, "Dopamine signaling modulates the stability and integration of intrinsic brain networks," *Cerebral Cortex*, vol. 29, no. 1, pp. 397–409, Jan. 2019.

[69] Y. Kunisato, Y. Okamoto, G. Okada, S. Aoyama, Y. Demoto, A. Munakata, M. Nomura, K. Onoda, and S. Yamawaki, "Modulation of default-mode network activity by acute tryptophan depletion is associated with mood change: A resting state functional magnetic resonance imaging study," *Neurosci. Res.*, vol. 69, no. 2, pp. 129–134, Feb. 2011.

[70] C. Scharinger, U. Rabl, C. H. Kasess, B. M. Meyer, T. Hofmaier, K. Diers, L. Bartova, G. Pail, W. Huf, and Z. Uzelac, "Platelet serotonin transporter function predicts default-mode network activity," *PLoS ONE*, vol. 9, no. 3, Mar. 2014, Art. no. e92543.

[71] M. C. McKinnon, K. Yucel, A. Nazarov, and G. M. MacQueen, "A meta-analysis examining clinical predictors of hippocampal volume in patients with major depressive disorder," *J. Psychiatry Neurosci.*, vol. 34, no. 1, pp. 41–54, 2009.

[72] M. J. Kempton, Z. Salvador, M. R. Munafò, J. R. Geddes, A. Simmons, S. Frangou, and S. C. Williams, "Structural neuroimaging studies in major depressive disorder: Meta-analysis and comparison with bipolar disorder," *Arch. Gen. Psychiatry*, vol. 68, no. 7, pp. 675–690, 2011.

[73] E. S. Brown, C. W. Hughes, R. McColl, R. Peshock, K. S. King, and A. J. Rush, "Association of depressive symptoms with hippocampal volume in 1936 adults," *Neuropsychopharmacology*, vol. 39, no. 3, pp. 770–779, Feb. 2014.

[74] Y.-J. Zhao, M.-Y. Du, X.-Q. Huang, S. Lui, Z.-Q. Chen, J. Liu, Y. Luo, X.-L. Wang, G. J. Kemp, and Q.-Y. Gong, "Brain grey matter abnormalities in medication-free patients with major depressive disorder: A meta-analysis," *Psychol. Med.*, vol. 44, no. 14, pp. 2927–2937, Oct. 2014.

[75] N. Jaworska, X.-R. Yang, V. Knott, and G. MacQueen, "A review of fMRI studies during visual emotive processing in major depressive disorder," *World J. Biol. Psychiatry*, vol. 16, no. 7, pp. 448–471, Oct. 2015.

[76] G. M. MacQueen, K. Yucel, V. H. Taylor, K. Macdonald, and R. Joffe, "Posterior hippocampal volumes are associated with remission rates in patients with major depressive disorder," *Biol. Psychiatry*, vol. 64, no. 10, pp. 880–883, Nov. 2008.

[77] H. Park, S. M. Sanchez, R. Kuplicki, A. Tsuchiyagaito, S. S. Khalsa, M. P. Paulus, and S. M. Guinjoan, "Attenuated interoceptive processing in individuals with major depressive disorder and high repetitive negative thinking," *J. Psychiatric Res.*, vol. 156, pp. 237–244, Dec. 2022.

[78] X. Cao, Z. Liu, C. Xu, J. Li, Q. Gao, N. Sun, Y. Xu, Y. Ren, C. Yang, and K. Zhang, "Disrupted resting-state functional connectivity of the hippocampus in medication-naïve patients with major depressive disorder," *J. Affect. Disorders*, vol. 141, nos. 2–3, pp. 194–203, Dec. 2012.

[79] L. Gong, Z. Hou, Z. Wang, C. He, Y. Yin, Y. Yuan, H. Zhang, L. Lv, H. Zhang, C. Xie, and Z. Zhang, "Disrupted topology of hippocampal connectivity is associated with short-term antidepressant response in major depressive disorder," *J. Affect. Disorders*, vol. 225, pp. 539–544, Jan. 2018.

[80] R. Ge, I. Torres, J. J. Brown, E. Gregory, E. McLellan, J. H. Downar, D. M. Blumberger, Z. J. Daskalakis, R. W. Lam, and F. Vila-Rodriguez, "Functional disconnectivity of the hippocampal network and neural correlates of memory impairment in treatment-resistant depression," *J. Affect. Disorders*, vol. 253, pp. 248–256, Jun. 2019.

[81] H. Long, Z. Chen, X. Xu, Q. Zhou, Z. Fang, M. Lv, X.-H. Yang, J. Xiao, H. Sun, and M. Fan, "Elucidating genetic and molecular basis of altered higher-order brain structure-function coupling in major depressive disorder," *NeuroImage*, vol. 297, Aug. 2024, Art. no. 120722.

[82] K. Bi, L. Hua, M. Wei, J. Qin, Q. Lu, and Z. Yao, "Dynamic functional–structural coupling within acute functional state change phases: Evidence from a depression recognition study," *J. Affect. Disorders*, vol. 191, pp. 145–155, Feb. 2016.

[83] M. S. Korgaonkar, A. N. Goldstein-Piekarski, A. Fornito, and L. M. Williams, "Intrinsic connectomes are a predictive biomarker of remission in major depressive disorder," *Mol. Psychiatry*, vol. 25, no. 7, pp. 1537–1549, Jul. 2020.

[84] V. Menon, "Large-scale brain networks and psychopathology: A unifying triple network model," *Trends Cognit. Sci.*, vol. 15, no. 10, pp. 483–506, Oct. 2011.

[85] B. T. Thomas Yeo, F. M. Krienen, J. Sepulcre, M. R. Sabuncu, D. Lashkari, M. Hollinshead, J. L. Roffman, J. W. Smoller, L. Zöllei, J. R. Polimeni, B. Fischl, H. Liu, and R. L. Buckner, "The organization of the human cerebral cortex estimated by intrinsic functional connectivity," *J. Neurophysiol.*, vol. 106, no. 3, pp. 1125–1165, Sep. 2011.

[86] L. Pasquini, S. L. Fryer, S. J. Eisendrath, Z. V. Segal, A. J. Lee, J. A. Brown, M. Saggar, and D. H. Mathalon, "Dysfunctional cortical gradient topography in treatment-resistant major depressive disorder," *Biol. Psychiatry: Cognit. Neurosci. Neuroimaging*, vol. 8, no. 9, pp. 928–939, Sep. 2023.

[87] J. R. Phillips, D. H. Hewedi, A. M. Eissa, and A. A. Moustafa, "The cerebellum and psychiatric disorders," *Frontiers Public Health*, vol. 3, p. 66, May 2015.

[88] L. Baldaçara, J. G. F. Borgio, A. L. T. D. Lacerda, and A. P. Jackowski, "Cerebellum and psychiatric disorders," *Revista Brasileira de Psiquiatria*, vol. 30, no. 3, pp. 281–289, Sep. 2008.

[89] B. M. Turner, S. Paradiso, C. L. Marvel, R. Pierson, L. L. B. Ponto, R. D. Hichwa, and R. G. Robinson, "The cerebellum and emotional experience," *Neuropsychologia*, vol. 45, no. 6, pp. 1331–1341, Jan. 2007.

[90] K. Heyder, B. Suchan, and I. Daum, "Cortico-subcortical contributions to executive control," *Acta Psychologica*, vol. 115, nos. 2–3, pp. 271–289, Feb. 2004.

[91] J. D. Bremner, M. Vythilingam, E. Vermetten, A. Nazeer, J. Adil, S. Khan, L. H. Staib, and D. S. Charney, "Reduced volume of orbitofrontal cortex in major depression," *Biol. Psychiatry*, vol. 51, no. 4, pp. 273–279, Feb. 2002.

[92] J. D. Schmahmann, "Disorders of the cerebellum: Ataxia, dysmetria of thought, and the cerebellar cognitive affective syndrome," *J. Neuropsychiatry*, vol. 16, no. 3, pp. 367–378, Aug. 2004.

[93] L. Liu, L.-L. Zeng, Y. Li, Q. Ma, B. Li, H. Shen, and D. Hu, "Altered cerebellar functional connectivity with intrinsic connectivity networks in adults with major depressive disorder," *PLoS ONE*, vol. 7, no. 6, Jun. 2012, Art. no. e39516.

[94] M. D. Greicius, B. H. Flores, V. Menon, G. H. Glover, H. B. Solvason, H. Kenna, A. L. Reiss, and A. F. Schatzberg, "Resting-state functional connectivity in major depression: Abnormally increased contributions from subgenual cingulate cortex and thalamus," *Biol. Psychiatry*, vol. 62, no. 5, pp. 429–437, Sep. 2007.

[95] Y. I. Sheline, J. L. Price, Z. Yan, and M. A. Mintun, "Resting-state functional MRI in depression unmasks increased connectivity between networks via the dorsal Nexus," *Proc. Nat. Acad. Sci. USA*, vol. 107, no. 24, pp. 11020–11025, Jun. 2010.

[96] M. E. Raichle, A. M. MacLeod, A. Z. Snyder, W. J. Powers, D. A. Gusnard, and G. L. Shulman, "A default mode of brain function," *Proc. Nat. Acad. Sci. USA*, vol. 98, no. 2, pp. 676–682, Jan. 2001.

[97] C. Habas, N. Kamdar, D. Nguyen, K. Prater, C. F. Beckmann, V. Menon, and M. D. Greicius, "Distinct cerebellar contributions to intrinsic connectivity networks," *J. Neurosci.*, vol. 29, no. 26, pp. 8586–8594, 2009.

[98] Y. Zheng, X. Chen, D. Li, Y. Liu, X. Tan, Y. Liang, H. Zhang, S. Qiu, and D. Shen, "Treatment-naïve first episode depression classification based on high-order brain functional network," *J. Affect. Disorders*, vol. 256, pp. 33–41, Sep. 2019.

[99] W. Guo, F. Liu, Y. Dai, M. Jiang, J. Zhang, L. Yu, L. Long, H. Chen, Q. Gao, and C. Xiao, "Decreased interhemispheric resting-state functional connectivity in first-episode, drug-naive major depressive disorder," *Prog. Neuro-Psychopharmacol. Biol. Psychiatry*, vol. 41, pp. 24–29, Mar. 2013.

[100] P. C. Mulders, P. F. van Eijndhoven, A. H. Schene, C. F. Beckmann, and I. Tendolkar, "Resting-state functional connectivity in major depressive disorder: A review," *Neurosci. Biobehavioral Rev.*, vol. 56, pp. 330–344, Sep. 2015.

[101] B. Wu, X. Li, J. Zhou, M. Zhang, and Q. Long, "Altered whole-brain functional networks in drug-Naïve, first-episode adolescents with major depression disorder," *J. Magn. Reson. Imag.*, vol. 52, no. 6, pp. 1790–1798, Dec. 2020.

[102] S. Campbell and G. MacQueen, "The role of the hippocampus in the pathophysiology of major depression," *J. Psychiatry Neurosci.*, vol. 29, no. 6, pp. 417–426, Nov. 2004.

[103] J. Cole, S. G. Costafreda, P. McGuffin, and C. H. Y. Fu, "Hippocampal atrophy in first episode depression: A meta-analysis of magnetic resonance imaging studies," *J. Affect. Disorders*, vol. 134, nos. 1–3, pp. 483–487, Nov. 2011.

[104] G. M. MacQueen, "Magnetic resonance imaging and prediction of outcome in patients with major depressive disorder," *J. Psychiatry Neurosci.*, vol. 34, no. 5, pp. 343–349, 2009.

[105] K. N. Ochsner and J. J. Gross, "The neural architecture of emotion regulation," *Handbook Emotion Regulation*, vol. 1, no. 1, pp. 87–109, 2007.

[106] N. Chen, J. Shi, Y. Li, S. Ji, Y. Zou, L. Yang, Z. Yao, and B. Hu, "Decreased dynamism of overlapping brain sub-networks in major depressive disorder," *J. Psychiatric Res.*, vol. 133, pp. 197–204, Jan. 2021.

[107] C.-G. Yan, X. Chen, L. Li, F. X. Castellanos, T.-J. Bai, Q.-J. Bo, J. Cao, G.-M. Chen, N.-X. Chen, and W. Chen, "Reduced default mode network functional connectivity in patients with recurrent major depressive disorder," *Proc. Nat. Acad. Sci. USA*, vol. 116, no. 18, pp. 9078–9083, Apr. 2019.

[108] H. Yang, X. Chen, Z.-B. Chen, L. Li, X.-Y. Li, F. X. Castellanos, T.-J. Bai, Q.-J. Bo, J. Cao, and Z.-K. Chang, "Disrupted intrinsic functional brain topology in patients with major depressive disorder," *Mol. psychiatry*, vol. 26, no. 12, pp. 7363–7371, Aug. 2021.

[109] X. Wang, J. Xia, W. Wang, J. Lu, Q. Liu, J. Fan, T. Soondrum, Q. Yu, C. Tan, and X. Zhu, "Disrupted functional connectivity of the cerebellum with default mode and frontoparietal networks in young adults with major depressive disorder," *Psychiatry Res.*, vol. 324, Jun. 2023, Art. no. 115192.

[110] Y.-D. Ding, X. Chen, Z.-B. Chen, L. Li, X.-Y. Li, F. X. Castellanos, T.-J. Bai, Q.-J. Bo, J. Cao, and Z.-K. Chang, "Reduced nucleus accumbens functional connectivity in reward network and default mode network in patients with recurrent major depressive disorder," *Transl. Psychiatry*, vol. 12, no. 1, p. 236, Jun. 2022.

[111] D. Zhi, V. D. Calhoun, L. Lv, X. Ma, Q. Ke, Z. Fu, Y. Du, Y. Yang, X. Yang, M. Pan, S. Qi, R. Jiang, Q. Yu, and J. Sui, "Aberrant dynamic functional network connectivity and graph properties in major depressive disorder," *Frontiers Psychiatry*, vol. 9, p. 339, Jul. 2018.

[112] D. Zhi, X. Ma, L. Lv, Q. Ke, Y. Yang, X. Yang, M. Pan, S. Qi, R. Jiang, Y. Du, Q. Yu, V. D. Calhoun, T. Jiang, and J. Sui, "Abnormal dynamic functional network connectivity and graph theoretical analysis in major depressive disorder," in *Proc. 40th Annu. Int. Conf. IEEE Eng. Med. Biol. Soc. (EMBC)*, Jul. 2018, pp. 558–561.

[113] C. Zhang, H. Jing, H. Yan, X. Li, J. Liang, Q. Zhang, W. Liang, Y. Ou, C. Peng, Y. Yu, W. Wu, G. Xie, and W. Guo, "Disrupted interhemispheric coordination of sensory-motor networks and insula in major depressive disorder," *Frontiers Neurosci.*, vol. 17, Mar. 2023, Art. no. 1135337.

[114] J. Liu, Y. Fan, L.-L. Zeng, B. Liu, Y. Ju, M. Wang, Q. Dong, X. Lu, J. Sun, L. Zhang, H. Guo, F. Zhao, W. Li, L. Zhang, Z. Li, M. Liao, Y. Zhang, D. Hu, and L. Li, "The neuroprogressive nature of major depressive disorder: Evidence from an intrinsic connectome analysis," *Transl. Psychiatry*, vol. 11, no. 1, p. 102, Feb. 2021.

[115] Y. Ding, Y. Ou, H. Yan, X. Fu, M. Yan, H. Li, F. Liu, and W. Guo, "Disrupted cerebellar-default mode network functional connectivity in major depressive disorder with gastrointestinal symptoms," *Frontiers Cellular Neurosci.*, vol. 16, Mar. 2022, Art. no. 833592.

[116] M. Yan, J. Chen, F. Liu, H. Li, R. Huang, Y. Tang, J. Zhao, and W. Guo, "Disrupted regional homogeneity in major depressive disorder with gastrointestinal symptoms at rest," *Frontiers Psychiatry*, vol. 12, May 2021, Art. no. 636820.

SEMEN A. KURKIN received the specialist degree in radiophysics and electronics and the Ph.D. degree in radiophysics from Saratov State University (SSU), Saratov, Russia, in 2008 and 2011, respectively.

From 2009 to 2018, he was an Associate Professor with SSU. From 2018 to 2019, he was a Professor with Saratov State Technical University, Saratov. From 2019 to 2021, he was a Professor with Innopolis University, Kazan, Russia. He is currently a Leading Researcher with the Baltic Center for Neurotechnology and Artificial Intelligence, Immanuel Kant Baltic Federal University, Kaliningrad, Russia. He has published more than 100 WoS/Scopus articles and continues his research in neuroscience, including multiple projects with international cooperation. His research interests include complex network theory, methods of brain diagnostics, development of AI methods for neuroimaging data processing, and applied research in neurotechnologies and education.

NIKITA M. SMIRNOV received the bachelor's degree in computer science from Innopolis University, Innopolis, Russia, in 2022, and the master's degree in pedagogy from Immanuel Kant Baltic Federal University (BFU), Kaliningrad, Russia, in 2024.

From 2021 to 2022, he was an Assistant Researcher with the Neuroscience and Cognitive Technologies Laboratory, Innopolis University. He is currently an Assistant Researcher with BFU. His research interests include complex network theory, methods of brain diagnostics, development of AI methods for neuroimaging data processing, and applied research in neurotechnologies and education.

ROSITSA PAUNOVA received the M.D. degree from the Medical University of Plovdiv, Bulgaria, in 2021. She is currently pursuing the Ph.D. degree in psychiatry and neuroscience.

Since 2022, she has been an Assistant Professor of psychiatry and medical psychology with the Medical University of Plovdiv. She has published more than 20 WoS/Scopus articles and continues her research in psychiatry and neuroscience, including multiple projects with international cooperation. Her research interests include psychiatry, neuroimaging in psychiatry, and development of AI methods for neuroimaging data processing.

SEVDALINA KANDILAROVA is a medically trained Psychiatrist, currently engaged with both teaching and research. She has been involved in the establishment of the research complex for translational neuroscience and since its official launch, in 2015, she has been the leading on-site Researcher developing and testing the paradigms for functional magnetic resonance imaging (fMRI). Since 2022, she has been an Associate Professor of psychiatry and medical psychology with the Medical University of Plovdiv, Bulgaria. She has been trained in Basel and Bergen to perform neuroimaging studies and to analyze structural and functional neuroimaging data. She has performed her own research project on depression leading to the Ph.D. degree, in 2017, and she is continuing with her postdoctoral training. She has been involved in several long-lasting collaborations with fMRI research groups at the University of Bergen and the University of Basel. She has published more than 47 WoS/Scopus articles and continues her research in neuroscience, including multiple projects with international cooperation. Her research interests include the application of structural, resting state, and task-related fMRI, as well as magnetic resonance spectroscopy for the differential diagnosis of major psychiatric disorders.

DROZDSTOY STOYANOV received the M.D. degree from the Medical University of Sofia, Bulgaria, in 2002, the Ph.D. degree in psychiatry and neurology, in 2007, the master's degree in philosophy and mental health, in 2010, and the Doctor of Medical Sciences degree in 2018.

He was a Board Certified Psychiatrist, in 2008. From 2008 to 2013, he was an Associate Professor with the Medical University of Plovdiv, Bulgaria. Since 2014, he has been a Full Professor and the Head of the Department of Psychiatry and Medical Psychology, since 2020; the Director of the Research Institute, Medical University in Plovdiv, since 2024. He has published more than 130 WoS/Scopus articles and continues his research in neuroscience, including multiple projects with international cooperation. His works received more than 3000 independent citations with an H-index=32. His research interests include translational neuropsychiatric imaging, philosophy, psychiatry, and psychology.

LARISA MAYOROVA received the M.D. degree from Lomonosov Moscow State University, in 2010, and the Ph.D. degree in neurophysiology, in 2013.

Board Certified Neurologist, in 2015. From 2013 to 2020, she was a Research Fellow with the Institute of Higher Nervous Activity and Neurophysiology, the Center for Speech Pathology and Neurorehabilitation, and the Solovyov Moscow Research and Practical Psychoneurological Center. She has been a Senior Research Fellow with the Institute of Higher Nervous Activity and Neurophysiology and the Federal Research and Clinical Center of Intensive Care Medicine and Rehabilitology, Moscow, since 2019, and the Head of the Laboratory of Experimental Neurology and Neuroimaging, since 2023. She has published more than 30 WoS/Scopus articles and continues her research in neuroscience. Her research interests include human neuroimaging studies investigating the mechanisms underlying chronic disorders of consciousness, post-stroke functional deficit, and brain stimulation.

ALEXANDER E. HRAMOV was born in Saratov, Russia, in September 1974. He received the specialist degree and Ph.D. degrees in electronic engineering from Saratov State University, Russia, in 1996 and 1999, respectively. In 2005, he defended his Ph.D. dissertation in mathematics and physics.

From 1999 to 2014, he held positions as a Researcher, an Associate Professor, and a Full Professor with Saratov State University, Russia. From 2014 to 2018, he was a Leading Researcher with the Science and Educational Center of Artificial Intelligence Systems and Neurotechnology, and the Head of the Department of Automation, Control, and Mechatronics, Saratov State Technical University, Russia. From 2019 to 2021, he was a Professor and the Head of the Laboratory of Neuroscience and Cognitive Technology, Innopolis University, Kazan, Russia. He is currently the Head of the Baltic Center for Neurotechnology and Artificial Intelligence, Immanuel Kant Baltic Federal University, Kaliningrad, Russia. His research interests include complex network theory, methods of brain diagnostics, development of AI methods for neuroimaging data processing, and applied research in digital medicine, neurotechnologies, and education.